Electronic Supplementary Material (ESI) for Polymer Chemistry.

Supplementary Information

6-Oxoverdazyl Radical Polymers with Tunable Electrochemical Properties

Jacquelyn T. Price,[ab] Joseph A. Paquette,[ab] Christopher S. Harrison,[ab] Reg Bauld,[bc] Giovanni Fanchini,[bc] and Joe B. Gilroy*[ab]*

[a]*Department of Chemistry, The University of Western Ontario, London N6A 5B7, ON, Canada.*

[b]*The Centre for Advanced Materials and Biomaterials Research (CAMBR), The University of Western Ontario, London N6A 5B7, ON, Canada.*

[c]*Department of Physics and Astronomy, The University of Western Ontario, London N6A 3K7, ON, Canada.*

Table of Contents

Experimental Details

General considerations

All reactions and manipulations were carried out under a nitrogen atmosphere using standard Schlenk or glove box techniques unless otherwise stated. Solvents were obtained from Caledon Laboratories, dried using an Innovative Technologies Inc. solvent purification system, collected under vacuum, and stored under a nitrogen atmosphere over 4 Å molecular sieves. All reagents were purchased from Sigma-Aldrich or Alfa Aesar and used as received unless otherwise stated. *p*-Benzoquinone was freshly sublimed *in vacuo* before use. 4-Methacryloyloxybenzaldehyde,[1] 4-pivaloyloxybenzaldehyde,[2] tetrazane **S1,**[3, 4] tetrazane **7c,**[3, 5] and 6-oxoverdazyl **8c**[3, 5] were prepared according to previously published procedures.

NMR Spectra were recorded on a 400 MHz (^{1}H: 399.8 MHz) and a 600 MHz (^{1}H: 599.5 MHz, ^{13}C{^{1}H}: 150.8 MHz) Varian INOVA instrument, or a 400 MHz (^{13}C: 100.6 MHz) Varian Mercury instrument. ^{1}H NMR spectra were referenced to $CHCl_3$ (7.26 ppm), CD_3SOCD_2H (2.50 ppm), or CD_2HCN (1.93 ppm) and ^{13}C{^{1}H} NMR spectra were referenced to $CDCl_3$ (77.2 ppm) or CD_3SOCD_3 (39.5 ppm). Mass spectrometry data were recorded in positive-ion mode using a high resolution Finnigan MAT 8200 spectrometer using electron impact ionization. UV-vis spectra were recorded in dichloromethane solutions and recorded using a Cary 300 Scan instrument. Four separate concentrations were run for each sample, and molar extinction coefficients were determined from the slope of a plot of absorbance against concentration. IR spectra were recorded as KBr pellets using a Bruker Vector 33 FT-IR spectrometer. Gel permeation chromatography (GPC) was carried out at a flow rate of 1 mL min^{-1} in *N,N*-dimethylformamide (DMF) with 10 mM LiBr and 1% (v/v) triethylamine added at a regulated temperature of 85 °C using a Waters 515 pump, equipped with a Wyatt Optilab REx detector and

two PLgel 5 μm mixed-D (300 mm × 7.5 mm) columns from Polymer Laboratories connected in series. Calibration was performed using monodisperse polystyrene standards supplied by Polymer Lab. Elemental analyses (C, H, N) were carried out by Laboratoire d'Analyse Élémentaire de l'Université de Montréal, Montréal, QC, Canada.

Electrochemical Methods

Cyclic voltammetry experiments were performed with a Bioanalytical Systems Inc. (BASi) Epsilon potentiostat and analyzed using BASi Epsilon software. Typical electrochemical cells consisted of a three-electrode setup including a glassy carbon working electrode, platinum wire counter electrode, and silver wire *pseudo*-reference electrode. Experiments were run at variable scan rates in degassed tetrahydrofuran (THF) solutions of the analyte (~1 mM) and electrolyte (0.1 M tetrabutylammonium hexafluorophosphate). Voltammograms were referenced against the ferrocene/ferrocenium redox couple (~1 mM internal standard) and corrected for internal cell resistance using the BASi Epsilon software.

Electron Paramagnetic Resonance (EPR) Spectroscopy

EPR measurements were made on *ca.* 10^{-5} M dichloromethane solutions of verdazyl radical polymers **6a,b** and verdazyl radicals **8a,b** that had been subjected to three freeze-pump-thaw cycles in 0.4 mm quartz tubes using a JEOL JES-FA200 EPR. All measurements were made at 20 °C and *g* factors were referenced relative to a built-in manganese dioxide marker within the resonant cavity of the instrument.

Kelvin Probe Force Microscopy (KPFM)

Thin films of polymer **6a** were prepared under atmospheric conditions using a Laurell WS40-6NPP spin coater from a 15 mg mL^{-1} solution in anhydrous chlorobenzene. A spinning speed of 1,000 RPM produced a polymeric thin film of approximately 166 ± 10 nm thickness. The topography and work function of thin films of 6-oxoverdazyl polymer **6a** were determined in one single scan by intermittent contact mode Atomic Force Microscopy (AFM) and Kelvin Probe Force Microscopy (KPFM), respectively. Images were recorded on a Witec Alpha 300S atomic force microscope specifically modified for KPFM experiments with the attachment of a Stanford DS 345 function generator. This generator is locked-in at the second-order resonance frequency of the AFM cantilever using a Stanford SR844-RF lock-in amplifier that transfers the data directly to the digital controller of the Witec system. The AFM/KPFM microscope is contained in a sealed enclosure for controlling the temperature and humidity of the atmosphere during measurements. For each pixel of an AC-mode AFM scan, the voltage V_{b0} resulting in the minimum force between the tip and the sample is optimized in the V_b = ± 10 V range using an integral-proportional feedback loop. Under those conditions, $e \cdot V_{b0}$ represents the work function of the sample relative to the tip.[6] Conducting cantilevers (≈75 kHz first-order resonance frequency, ≈425 kHz second-order resonance frequency, from Nanosensors Inc.) were used for AFM/KPFM imaging. For KPFM, the work function of the polymeric thin film was determined from its shift from the work function of ITO recorded on a portion of the sample in which the polymer film was removed. The work function of the used ITO reference was assumed to be 4.7 eV.[7] In order to determine the uncertainty associated with such a work function estimate, the conducting AFM tip was also calibrated by scanning highly doped p- and n-type silicon wafers of known work functions and determined to be ≈4.6 ± 0.1 eV. With this crosscheck we

determined the uncertainty associated to our KPFM measurements to be ± 0.1 eV, or better. KPFM histograms were directly extracted from the recorded images using the Witec Project 2.04 software and analyzed using a model comprising three Gaussian peaks, one for the signal from the polymeric film surface, one for the signal from the ITO film surface and one minor peak related to the signal related to the edge of the film, as shown in the inset of Fig. 3.

X-ray Crystallography Details

Crystals suitable for X-ray diffraction were grown by slow cooling (–20 °C) a saturated toluene solution of **8a**, slow cooling (–20 °C) a saturated ethyl acetate solution of **8c**, or vapor diffusion of diethyl ether into a saturated acetonitrile solution of **9c** at –35 °C. X-ray diffraction data were collected on a Nonius KappaCCD or a Bruker ApexII CCD area detector using graphite-monochromated Mo Kα radiation (λ = 0.71073 Å). Single crystals were selected under Paratone-N, mounted on Mitegen polyimide micromount, and immediately placed under a cold stream of N_2. Structures were solved by direct methods and refined using full-matrix least squares on F^2.[8] See Table S1 for crystallographic data and the CCDC (991914–991916) for structural data.

Table S1 Crystallographic data for compounds **8a**, **8c**, and **9c**.

	8a	**8c**	**9c**
Chemical Formula	$C_{19}H_{27}N_4O_3$	$C_{14}H_{19}N_4O$	$C_{14}H_{19}BFN_4O$
FW (*g/mol*)	359.44	259.33	346.14
Crystal Dimensions (*mm*)	0.51 x 0.17 x 0.052	0.4 x 0.3 x 0.3	0.24 x 0.22 x 0.18
Crystal Habit	Red, block	Red, block	Red, block
Crystal System	Monoclinic	Orthorhombic	Monoclinic
Space Group	*P* $2_1/c$	*P* $na2_1$	*P* $2_1/c$
Temperature (K)	110	150(2)	150(2)
a (Å)	18.930(7)	16.219(7)	8.1059(16)
b (Å)	5.8718(19)	15.484(9)	13.501(5)
c (Å)	18.364(5)	5.7192(14)	15.435(6)
α (°)	90	90	90
β (°)	105.364(12)	90	99.864(10)
γ (°)	90	90	90
V ($Å^3$)	1968.3(11)	1436.4(11)	1664.3(10)
Z	4	4	4
ρ (*g/cm*)	1.213	1.199	1.381
λ, Å, (Mo Kα)	0.71073	0.71073	0.71073
μ (cm^{-1})	0.084	0.079	0.119
Diffractometer Type	Bruker APEX-II CCD	Nonius KappaCCD	Nonius KappaCCD
R_{merge}	0.0548	0.0269	0.0376
[a]R_1 [I > 2]	0.0515	0.0313	0.0580
[b]*w*R_2 [I > 2]	0.1282	0.0735	0.1489
R_1 (all data)	0.0891	0.0378	0.0818
wR_2 (all data)	0.1527	0.0767	0.1685
GOF	1.041	1.045	1.048

[a]$R_1 = \Sigma(|F_o| - |F_c|) / \Sigma F_o$

[b]$wR_2 = [\Sigma(w(F_o^2 - F_c^2)^2) / \Sigma(w F_o^4)]^{½}$

GOF = $[\Sigma(w(F_o^2 - F_c^2)^2) / (\text{No. of reflns.} - \text{No. of params.})]^{½}$

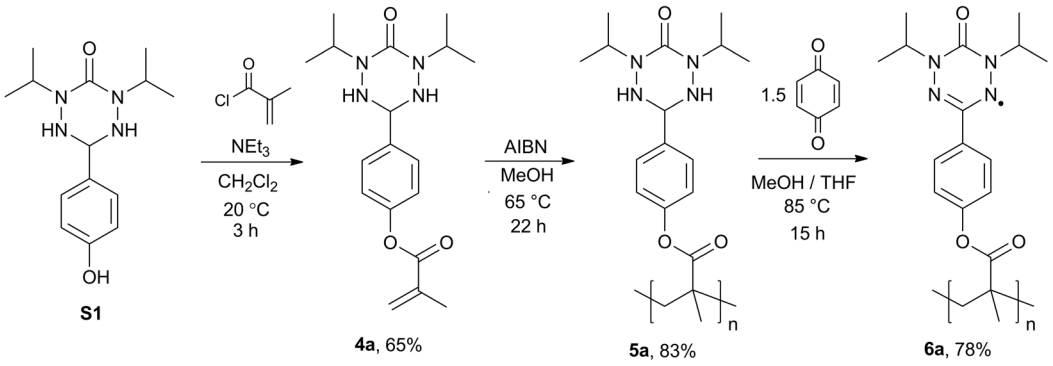

Synthesis of 1,5-di-*iso*propyl-3-(4-phenylmethacryloyl)-6-oxotetrazane 4a

A sample of tetrazane **S1** (2.20 g, 7.90 mmol) was added to a Schlenk flask equipped with stir bar and combined with dry dichloromethane (150 mL) and dry triethylamine (1.1 mL, 0.79 g, 7.9 mmol). Methacryloyl chloride (0.70 mL, 0.75 g, 7.9 mmol) was then added dropwise via syringe to the suspension of tetrazane **S1** causing dissolution. After stirring for 3 h at 20 °C, deionized water (10 mL) was transferred to the reaction flask via syringe and the reaction mixture was stirred for 5 min to consume any remaining methacryloyl chloride. The reaction mixture was then transferred to a separatory funnel and washed with deionized water (3 x 100 mL). The organic layer was dried over magnesium sulfate before the solvent was removed to yield a light yellow powder. Recrystallization from a saturated ethyl acetate solution afforded tetrazane **4a** as a soft, fibrous white solid. Yield = 1.75 g, 65%. ^{1}H NMR (400.1 MHz, d_6-DMSO): δ 7.61 (d, 2H, $^{3}J_{HH}$ = 8 Hz, aryl C*H*), 7.20 (d, 2H, $^{3}J_{HH}$ = 8 Hz, aryl C*H*), 6.28 (s, 1H, =C*H*), 5.91 (s, 1H, =C*H*), 5.00 (d, 2H, $^{3}J_{HH}$ = 12 Hz, N*H*), 4.50 (sept, 1H, $^{3}J_{HH}$ = 7 Hz, C*H*), 4.39 (t, 1H, $^{3}J_{HH}$ = 12 Hz, C*H*), 2.00 (s, 3H, C*H*$_3$), 1.07 (d, 6H, $^{3}J_{HH}$ = 7 Hz, C*H*$_3$), 1.04 (d, 6H, $^{3}J_{HH}$ = 7 Hz, C*H*$_3$). ^{13}C{^{1}H} NMR (100.6 MHz, d_6-DMSO): δ 165.3, 153.4, 150.4, 135.2, 134.1, 127.9, 121.7, 71.1, 46.7, 19.5, 18.4, 18.0. FT-IR (ranked intensity), KBr pellet: 724(10), 916(7), 1129(2), 1205(9), 1317(8), 1429(6), CO tetrazane 1583(1), CO ester 1735(3), 2977(4), NH tetrazane 3232(5) cm^{-1}. Mass Spec. (EI, +ve mode): exact mass calculated for $C_{18}H_{26}N_4O_3$:

346.2005; found: 346.1992; difference: –3.8 ppm. Anal. Calcd. (%) for $C_{18}H_{26}N_4O_3$: C, 62.41; H, 7.56; N, 16.17. Found: C, 62.40; H, 7.61; N, 16.01.

Synthesis of *iso*propyl-substituted tetrazane polymer 5a

To a sample of tetrazane **4a** (3.0 g, 8.64 mmol) was added degassed methanol (15 mL) in a greaseless Schlenk flask equipped with a stir bar under nitrogen. Azobisisobutylnitrile (AIBN) (0.075 g, 0.43 mmol) was added to the reaction flask under a flow of nitrogen and the reaction mixture was further degassed by 2 more freeze-pump-thaw cycles. The reaction was then heated to 65 ºC for 22 h at which time the solvent was removed *in vacuo* yielding a white solid. The white solid was then washed with ethyl acetate (3 x 30 mL) to remove trace amounts of tetrazane **4a**. Tetrazane polymer **5a** was isolated as a white solid by centrifugation and dried at 20 °C *in vacuo* for 16 h before it was stored at 5 ºC to avoid undesirable oxidation. Yield = 2.47 g, 83%. ^{1}H NMR (400.1 MHz, d_6-DMSO): 7.57 (br, s, 2H, aryl C*H*), 7.15 (br, s, 2H, aryl C*H*), 4.97 (br, s, 2H, N*H*), 4.45 (br, s, 2H, C*H*(CH_3)), 4.35 (br, s, 1H, C*H*), 2.50–2.20 overlaps residual NMR solvent signal (v. br, s, 2H, CH_2), 1.41–1.33 (br, m, 3H, CH_3), 0.99 (br, s, 12H, CH_3). FT-IR (ranked intensity), KBr pellet: 728(8), 879(5), 1017(9), 1166(2), 1416(4), 1507(10), CO tetrazane 1613(1), CO ester 1751(6), 2917(3), NH tetrazane 3244(7) cm^{-1}. GPC: M_n = 25,260 Da, M_w = 46,230 Da, PDI = 1.83. Anal. Calcd. (%) for $[C_{18}H_{26}N_4O_3]_n$: C, 62.41; H, 7.56; N, 16.17. Found: C, 61.75; H, 7.64; N, 15.91.

Synthesis of *iso*propyl-substituted 6-oxoverdazyl polymer 6a

A sample of **5a** (1.50 g, 4.30 mmol) and *p*-benzoquinone (0.72 g, 6.6 mmol) were added to a mixture of tetrahydrofuran (30 mL) and methanol (30 mL) and heated to 85 ºC for 15 h. Upon

heating, the reaction mixture changed from yellow to bright red/orange in colour. The reaction was cooled to 20 °C and concentrated *in vacuo*. The resulting red residue was taken up in dichloromethane (60 mL) and purified by column chromatography (neutral alumina, dichloromethane eluent). The orange solution was then collected and concentrated *in vacuo.* The polymer was further purified by precipitating (in triplicate) concentrated dichloromethane solutions into pentane. 6-Oxoverdazyl polymer **6a** was isolated as an orange solid by centrifugation and dried at 35 ºC under reduced pressure for 16 h. Yield = 1.15 g, 78%. FT-IR (ranked intensity), KBr pellet: 657(8), 877(9), 722(6), 1016(7), 1164(2), 1387(3), 1510(5), CO verdazyl 1685(1), CO ester 1753(10), 2979(4) cm^{-1}. UV-vis (CH_2Cl_2): λ_{max} 417 nm (ε = 1,650 M^{-1} cm^{-1}). GPC: M_n = 25,750 Da, M_w = 48,670 Da, PDI = 1.89. Anal. Calcd. (%) for $[C_{18}H_{23}N_4O_3]_n$: C, 62.96; H, 6.75; N, 16.32. Found: C, 60.62; H, 6.16; N, 15.75.

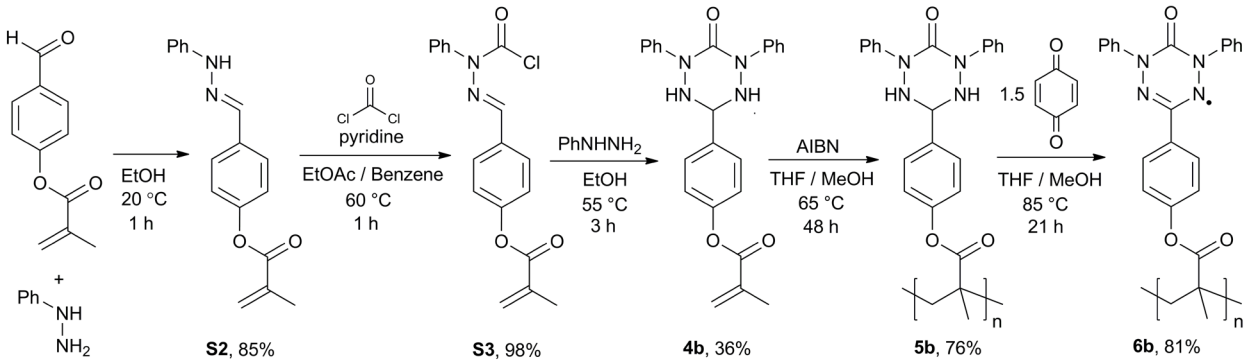

Synthesis of 4-methacryloylbenzaldehyde phenylhydrazone S2

The preparation was adapted from a procedure by Milcent and coworkers.[9] To a solution of 4-formylphenyl methacrylate (4.00 g, 21.0 mmol) in ethanol (50 mL) was added phenylhydrazine (2.49 mL, 2.73 g, 25.2 mmol). A yellow precipitate quickly formed, and the reaction was left to stir for 1 h at 20 °C. The solution was poured into ice-cold water (200 mL). The white precipitate was filtered before it was recrystallized in 2-propanol to give **S2** as lustrous white

crystals. Yield = 5.01 g, 85%. ^{1}H NMR (599.5 MHz, d_6-DMSO): δ 10.36 (s, 1H, N*H*), 7.89 (s, 1H, N=C*H*), 7.70 (d, 2H, $^{3}J_{HH}$ = 9 Hz, aryl C*H*), 7.22 (m, 4H, aryl C*H*), 7.09 (d, 2H, $^{3}J_{HH}$ = 7 Hz, aryl C*H*), 6.75 (t, 1H, $^{3}J_{HH}$ = `7 Hz, aryl C*H*), 6.29 (s, 1H, C=CH_2), 5.90 (s, 1H, C=CH_2), 2.01 (s, 3H, CH_3). ^{13}C{^{1}H} NMR (150.8 MHz, *d*6-DMSO): δ 165.2, 150.1, 145.2, 135.5, 135.2, 133.6, 129.1, 127.7, 126.5, 122.0, 118.8, 112.0, 18.0. Mass Spec. (EI, +ve mode): exact mass calculated for $C_{17}H_{16}N_2O_2$: 280.1212; exact mass found: 280.1211; difference: +0.43 ppm.

Synthesis of 4-methacryloylbenzaldehyde α-chloroformylphenylhydrazone S3

This procedure was adapted from a preparation by Milcent and coworkers.[9] To a 0 °C solution of phosgene (2.94 mL, 4.46 mmol, 15 wt % in toluene) was added dropwise hydrazone **S2** (1.00 g, 3.57 mmol) dissolved in a minimum amount of dry ethyl acetate/benzene (1:1, 20 mL) containing dry pyridine (0.32 mL, 0.33 g, 3.9 mmol) under N_2. Once the addition was complete, the pink mixture was heated to 60 °C for 1 h. The solvent was then removed *in vacuo.* The pink impurity was removed by column chromatography (silica gel, dichloromethane eluent). The resulting solid was recrystallized in cyclohexane to give **S3** as a white microcrystalline solid. Yield = 1.19 g, 98%. ^{1}H NMR (399.8 MHz, $CDCl_3$): δ 7.67 (m, 2H, aryl C*H*), 7.56 (m, 3H, aryl C*H*), 7.32 (s, 1H, N=C*H*), 7.26 (m, 2H, aryl C*H*), 7.15 (m, 2H, aryl C*H*), 6.34 (s, 1H, C=CH_2), 5.77 (m, 1H, C=CH_2), 2.04 (s, 3H, CH_3). ^{13}C{^{1}H} NMR (100.6 MHz, $CDCl_3$): δ 165.3, 152.6, 144.7 (bs, *C*OCl), 135.9, 135.5, 130.8, 130.5, 130.2, 128.8, 128.7, 127.6, 122.0, 18.2. Note: The ^{13}C{^{1}H} NMR spectra were initially recorded in *d*6-DMSO, which resulted in rapid decomposition of product. Therefore, $CDCl_3$ was used, but this caused broadening of several signals and certain peaks could not be resolved. Mass Spec. (EI, +ve mode): exact mass calculated for $C_{18}H_{15}ClN_2O_3$: 342.0771; exact mass found: 342.0769; difference: –0.68 ppm.

Synthesis of 1,5-diphenyl-3-(4-phenylmethacryloyl)-6-oxotetrazane 4b

This procedure was adapted from a previous synthesis by Milcent and coworkers.[9] To a stirred solution of phenylhydrazine (0.23 mL, 0.25 g, 2.3 mmol) in ethanol (10 mL) was added the α-chloroformylphenylhydrazone **S3** (0.40 g, 1.2 mmol) in small portions over 15 min. After the addition was complete, the solution was heated to 55 °C and left to stir for 3 h. The solution began clear and became opaque as the reaction proceeded. The warm mixture was then poured into ice cold water (30 mL). The precipitate was filtered, dried *in vacuo* overnight and the grey solid was recrystallized in *n*-propanol to give **4b** as a white powder. Yield = 0.31 g, 64%. ^{1}H NMR (399.8 MHz, d_6-DMSO): δ 7.60 (m, 6H, aryl C*H*), 7.33 (t, 4H, $^{3}J_{HH}$ = 7 Hz, aryl C*H*), 7.17 (d, 2H, $^{3}J_{HH}$ = 9 Hz, aryl C*H*), 7.08 (t, 2H, $^{3}J_{HH}$ = 7 Hz, aryl C*H*), 6.43 (d, 2H, $^{3}J_{HH}$ = 9, N*H*), 6.27 (s, 1H, C=CH_2), 5.89 (s, 1H, C=CH_2), 5.42 (t, 1H, $^{3}J_{HH}$ = 9 Hz, N-C*H*), 1.99 (s, 3H, CH_3). ^{13}C{^{1}H} NMR (100.5 MHz, d_6-DMSO): δ 165.6, 157.4, 150.8, 143.1, 135.7, 135.6, 128.6, 128.4, 128.2, 123.7, 122.1, 121.5, 72.8, 18.4. FT-IR (ranked intensities) KBr pellet: 692(10), 742(11), 922(12), 1124(3), 1167(4), 1310(6), 1202(7), 1375(2), 1501(8), CO tetrazane 1625(1), CO ester 1735(5), NH tetrazane 3233(9) cm^{-1}. Mass Spec. (EI, +ve mode): exact mass calculated for $C_{24}H_{22}N_4O_3$: 414.1692; exact mass found: 414.1682; difference: –2.4 ppm. Anal. Calcd. (%) for $C_{24}H_{22}N_4O_3$: C, 69.55; H, 5.35; N, 13.52. Found: C, 69.20; H, 5.39; N, 13.40.

Synthesis of phenyl-substituted tetrazane polymer 5b

A dry solution of THF/MeOH (1:1, 10 mL) was degassed using the freeze-pump-thaw technique 3 times, followed by the addition of AIBN (0.050 g, 0.30 mmol, 5 mol %) to THF. A 2 mL aliquot of this AIBN solution was then transferred to a greaseless Schlenk flask containing tetrazane **4b** (0.50 g, 1.21 mmol). The mixture was shielded from light and heated to 65 °C in a

temperature controlled oil bath in a sealed flask and stirred for 48 h. The solution was removed from the oil bath and precipitated into ethyl acetate (3 x 20 mL), then dried *in vacuo* to afford **5b** as a white solid. Yield = 0.38 g, 76%. ^{1}H NMR (599.4 MHz, *d*6-DMSO): δ 7.55 (bs, 6H, aryl C*H*), 7.22 (bs, 4H, aryl C*H*), 7.01 (bs, 4H, aryl C*H*), 6.35 (bs, 2H, N*H*), 5.32 (bs, 1H, C*H*), 2.21 (bs, 2H, CH_2), 1.27 (bs, 3H, CH_3). FT-IR (ranked intensities) KBr pellet: 692(10), 756(9), 883(12), 1105(7), 1166(3), 1363(2), 1497(1), 1596(8), CO tetrazane 1666(5), CO ester 1750(4), NH tetrazane 3248(11) cm^{-1}. GPC: M_n = 20,280 Da, M_w = 25,450 Da, PDI = 1.49. Anal. Calcd. (%) for $[C_{24}H_{22}N_4O_3]_n$: C, 69.55; H, 5.35; N, 13.52 Found: C, 69.33; H, 5.44; N, 13.52.

Synthesis of phenyl-substituted 6-oxoverdazyl polymer 6b

A sample of **5b** (0.15 g, 0.36 mmol) and freshly sublimed *p*-benzoquinone (0.060 g, 0.54 mmol) were dissolved in tetrahydrofuran (20 mL). Once dissolved, methanol (10 mL) was added and the solution was heated to 85 ºC for 21 h. Upon heating, the reaction mixture changed from yellow to dark red. The reaction was cooled to 20 °C and concentrated *in vacuo*. The resulting red residue was taken up in dichloromethane (10 mL) and purified by column chromatography (neutral alumina, dichloromethane followed by tetrahydrofuran as eluent). The second fraction, a dark red solution, was collected and concentrated *in vacuo*. The solid was further dried at 40 °C *in vacuo* for 36 h, to obtain **6b** as a dark red solid. Yield = 0.12 g, 81%. FT-IR (ranked intensities) KBr pellet: 688(9), 748(8), 1101(3), 1162(2), 1266(4), 1251(7), 1464(5), CO verdazyl 1701(1), CO ester 1750(6), 2953(10) cm^{-1}. UV-vis (CH_2Cl_2): λ_{max} 566 nm (ε = 1,670 M^{-1} cm^{-1}), 319 nm (ε = 9,760 M^{-1} cm^{-1}), 262 nm (ε = 21,310 M^{-1} cm^{-1}). GPC: M_n = 12,000 Da, M_w = 14,500 Da, PDI = 1.46. Anal. Calcd. (%) for $[C_{24}H_{19}N_4O_3]_n$: C, 70.06; H, 4.65; N, 13.62. Found: C, 70.51; H, 5.44; N, 12.01.

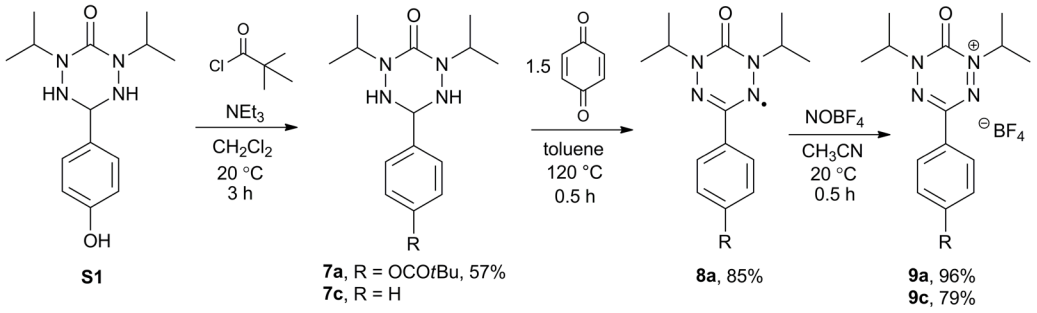

Synthesis of 1,5-diisopropyl-3-(4-trimethylacetylphenyl)-6-oxotetrazane 7a

A sample of tetrazane **S1** (2.80 g, 10.1 mmol) was added to a Schlenk flask equipped with a stir bar and combined with dichloromethane (200 mL) and triethylamine (1.41 mL, 1.02 g, 10.1 mmol). Trimethylacetyl chloride (1.24 mL, 1.21 g, 10.1 mmol) was then added dropwise via syringe to the suspension of tetrazane **S1** causing complete dissolution after a few min. After stirring for 3 h at 20 °C, deionized water (10 mL) was transferred to the reaction flask via syringe and the mixture was allowed to stir for 5 min to ensure any remaining trimethylacetyl chloride was consumed. The reaction mixture was transferred to a separatory funnel and washed with deionized water (3 x 100 mL). The organic layer was dried over magnesium sulfate before the solvent was removed *in vacuo* to yield a light yellow powder. Recrystallization from a saturated ethyl acetate solution afforded tetrazane **7a** as an off-white solid. Yield = 2.08 g, 57%. ^{1}H NMR (400.1 MHz, d_6-DMSO): δ 7.59 (d, 2H, $^{3}J_{HH}$ = 8 Hz, aryl C*H*), 7.12 (d, 2H, $^{3}J_{HH}$ = 8 Hz, aryl C*H*), 4.99 (d, 2H, $^{3}J_{HH}$ = 11 Hz, N*H*), 4.50 (sept. 2H, $^{3}J_{HH}$= 6.61 Hz, C*H*), 4.39 (t, 1H, $^{3}J_{HH}$ = 11 Hz, C*H*), 1.31 (s, 9H, CH_3), 1.05 (d, 6H, $^{3}J_{HH}$ = 7 Hz, CH_3), 1.03 (d, 6H, $^{3}J_{HH}$ = 7 Hz, CH_3). ^{13}C{^{1}H} NMR (100.6 MHz, d_6-DMSO): δ 176.6, 153.6, 150.8, 134.2, 128.1, 121.7, 71.3, 46.9, 26.9, 19.7, 18.6. FT-IR (ranked intensity), KBr pellet: 619(7), 640(10), 726(5), 894(3), 1115(4), 1426(8), CO tetrazane 1579(1), CO ester 1751(9), 2975(2), NH tetrazane 3236(6) cm^{-1}. Mass Spec. (EI, +ve mode): exact mass calculated for $C_{19}H_{30}N_4O_3$: 362.2318; exact mass found:

362.2315; difference: –0.8 ppm. Anal. Calcd. (%) for $C_{19}H_{30}N_4O_3$: C, 62.96; H, 8.34; N, 15.46. Found: C, 62.95; H, 8.44; N, 15.44.

Synthesis of 1,5-di-*iso*propyl-3-(4-trimethylacetylphenyl)-6-oxoverdazyl 8a

A sample of tetrazane **7a** (2.40 g, 6.20 mmol) was combined with freshly sublimed *p*-benzoquinone (1.08 g, 9.40 mmol) in a 250 mL round bottom flask equipped with a stir bar and a reflux condenser. To this flask, toluene (35 mL) was added before it was immersed in an oil bath, stirred, and heated at 120 °C for 30 min. The orange-red reaction mixture was cooled to 20 °C causing *p*-hydroquinone to precipitate from solution. The reaction mixture was filtered and the toluene removed from the filtrate *in vacuo* to afford an orange-red residue. Purification via flash column chromatography (neutral alumina, toluene eluent) followed by removal of the solvent afforded 6-oxoverdazyl **8a** as a bright orange microcrystalline solid. Yield = 1.90 g, 85%. FT-IR (ranked intensity), KBr: 658(9), 720(8), 895(10), 1116(2), 1165(7), 1227(4), 1366(3), CO verdazyl 1681(1), CO ester 1757(6), 2983(5) cm^{-1}. UV-vis (CH_2Cl_2): λ_{max} 417 nm (ε = 1,650 M^{-1} cm^{-1}). Mass Spec. (EI, +ve mode): exact mass calculated for $C_{19}H_{27}N_4O_3$: 359.2083; exact mass found: 359.2078; difference –1.4 ppm. Anal. Calcd. (%) for $C_{19}H_{27}N_4O_3$: C, 63.49; H, 7.57; N, 15.59. Found: C, 63.65; H, 7.76; N, 15.33.

Synthesis of 1,5-di-*iso*propyl-3-(4-trimethylacetylphenyl)-6-oxotetrazinium cation 9a

A sample of 6-oxoverdazyl **8a** (0.40 g, 1.10mmol) was added to a 20 mL glass vial equipped with a stir bar and dissolved in 3 mL of acetonitrile. An acetonitrile (5 mL) solution of $NOBF_4$ (0.13 g, 1.1 mmol) was then added dropwise to the reaction mixture over 5 min. During the reaction, the mixture changed from dark red to dark purple and the evolution of $NO_{(g)}$ was

observed. The reaction mixture stirred at 20 °C for 30 min and then concentrated *in vacuo*. The resulting purple powder was washed with ether (3 x 10 mL) and then concentrated affording tetrazinium cation **9a** as a dark purple solid. Yield: 0.47 g, 96%; ^{1}H NMR (400.1 MHz, $CDCl_3$): δ 7.97 (br s, 2H, aryl C*H*), 7.20 (br s, 3H, aryl C*H*), 5.23 (br s, 2H, $(CH_3)_2CH$), 1.52 (br s, 12H, CH_3), 1.38 (s, 9H, CH_3); ^{19}F NMR (376.1 MHz, $CDCl_3$): δ –153.4; ^{11}B NMR (128.3 MHz, $CDCl_3$): δ –2.1. FT-IR (ranked intensity), KBr pellet: 657(4), 789(9), 899(5), 1118(1), 1209(10), 1277(8), 1402(3), CO tetrazinium cation 1605(7), CO ester 1751(2), 2975(6) cm^{-1}. UV-vis (CH_2Cl_2): λ_{max} 287 nm (ε = 21,440 M^{-1} cm^{-1}), 355 nm (ε = 3,060 M^{-1} cm^{-1}), 530 nm (ε = 1,630 M^{-1} cm^{-1}). Mass Spec. (EI, +ve mode): exact mass calculated for $C_{19}H_{27}N_4O_3$: 359.2083; exact mass found: 359.2074; difference: +2.5 ppm. Anal. Calcd. (%) for $C_{19}H_{27}B_1F_4N_4O_3$: C, 51.14; H, 6.10; N, 12.56. Found: C, 50.15; H, 6.20; N, 12.78.

Synthesis of 1,5-di-*iso*propyl-3-phenyl-6-oxotetrazinium cation 9c

A sample of 6-oxoverdazyl **8c** (0.30 g, 1.14 mmol) was added to a 20 mL glass vial equipped with a stir bar and dissolved in 3 mL of acetonitrile. An acetonitrile (5 mL) solution of $NOBF_4$ (0.13 g, 1.1 mmol) was then added dropwise to the reaction mixture over 5 min. During the reaction, the mixture changed from dark red to dark purple and the evolution of $NO_{(g)}$ was observed. The reaction mixture stirred at 20 °C for 30 min and then concentrated *in vacuo*. The resulting bright orange powder was washed with ether (3 x 10 mL) and then concentrated affording tetrazinium cation **9c** as a bright orange/red powder. Yield: 0.32 g, 79%; ^{1}H NMR (400.1 MHz, CD_3CN, 40 °C): δ 8.22 (br s, 2H, aryl C*H*), 7.76 (br s, 3H, aryl C*H*), 5.41 (br s, 2H, $(CH_3)_2CH$), 1.62 (br s, 12H, CH_3); ^{19}F NMR (376.1 MHz, CD_3CN, –40 °C): δ 151.3; ^{11}B NMR (128.3 MHz, CD_3CN, 40 °C): δ 1.4. FT-IR (ranked intensities), KBr pellet: 659(8), 692(5),

782(4), 900(9), 1037(1), 1276(6), 1400(3), CO tetrazinium 1603(10), 751(2), 998(7) cm^{-1}. UV-vis (CH_2Cl_2): λ_{max} 280 nm (ε = 14,740 M^{-1} cm^{-1}), 350 nm (ε = 1,850 M^{-1} cm^{-1}), 510 nm (ε = 1590 M^{-1} cm^{-1}). Mass Spec. (EI, +ve mode): exact mass calculated for $C_{14}H_{10}N_4O_1$: 259.1559 exact mass found: 259.1562; difference: –1.15 ppm. Anal. Calcd. (%) for $C_{14}H_{19}B_1F_4N_4O_1$: C, 48.58; H, 5.53; N, 16.19. Found: C, 48.65; H, 5.65; N, 16.19.

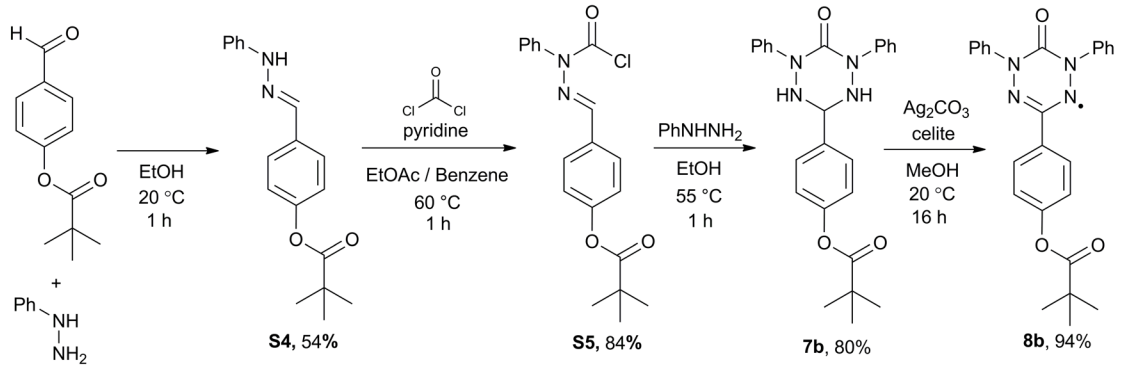

Synthesis of 4-pivaloylbenzaldehyde phenylhydrazone S4

The preparation was adapted from a procedure by Milcent and coworkers.[9] To a solution of 4-formylphenyl methacrylate (3.00 g, 14.6 mmol) in ethanol (50 mL) was added phenylhydrazine (1.72 mL, 18 g, 17.5 mmol). A yellow precipitate quickly formed, and the reaction was left to stir for 1 h at 20 °C. The solution was poured into ice-cold water (200 mL). The grey precipitate was filtered before it was recrystallized in 2-propanol to give **S4** as an off-white solid. Yield = 2.34 g, 54%. ^{1}H NMR (399.8 MHz, d_6-DMSO): δ 10.36 (s, 1H, N*H*), 7.89 (s, 1H, N=C*H*), 7.69 (d, 2H, $^3J_{HH}$ = 8.6 Hz, aryl C*H*), 7.23 (m, 2H, aryl C*H*), 7.10 (m, 2H, aryl C*H*), 6.76 (t, 1H, $^3J_{HH}$ = 7, aryl C*H*), 1.31 (s, 9H, CH_3). ^{13}C{^{1}H} NMR (100.5 MHz, d_6-DMSO): δ 176.3, 150.3, 145.2, 135.5, 135.5, 133.5, 129.1, 126.5, 126.4, 121.9, 118.7, 112.0, 38.5, 26.8, 26.7. Three extra signals present in the ^{13}C{^{1}H} NMR due to restricted rotation of phenylpivalate moiety. Mass

Spec. (EI, +ve mode): exact mass calculated for $C_{18}H_{20}N_2O_2$: 296.1525; exact mass found: 296.1531; difference: +2.03 ppm.

4-pivaloylbenzaldehyde α-chloroformylphenylhydrazone S5

This procedure was adapted from a preparation by Milcent and coworkers.[9] To a 0 °C solution of phosgene (4.17 mL, 6.33 mmol, 15 wt % in toluene) was added dropwise phenylhydrazone **S4** (1.50 g, 5.06 mmol) that was dissolved in minimum amount of dry ethyl acetate/benzene (1:1, 20 mL) with distilled pyridine (0.45 mL, 0.44 g, 5.6 mmol) under N_2. Once the addition was complete, the pink mixture was heated to 60 °C for 1 h. The solvent was then removed *in vacuo.* The pink impurity was removed by column chromatography (silica gel, dichloromethane eluent). The clear colourless oil was precipitated in ethanol, followed by recrystallization in ethanol to give **S5** as a white solid. Yield = 1.53 g, 84%. ^{1}H NMR (399.8 MHz, $CDCl_3$): δ 7.67 (d, 2H, $^3J_{HH}$ = 9 Hz, aryl C*H*), 7.59 (m, 3H, aryl C*H*), 7.33 (s, 1H, N=C*H*), 7.28 (d, 2H, $^3J_{HH}$ = 7.43 Hz, aryl C*H*), 7.09 (d, 2H, $^3J_{HH}$ = 9 Hz, aryl C*H*), 1.36 (s, 9H, (CH_3)$_3$). ^{13}C{^{1}H} NMR (100.6 MHz, $CDCl_3$): δ 176.6, 153.0, 144.9 (bs, *C*OCl), 136.1, 130.7, 130.5, 130.2, 128.9, 122.0, 39.1, 27.0. Note: The ^{13}C{^{1}H} NMR spectra were initially recorded in *d*6-DMSO, which resulted in rapid decomposition of product. Therefore, $CDCl_3$ was used, but this caused broadening of several signals and certain peaks could not be resolved. Mass Spec. (EI, +ve mode): exact mass calculated for $C_{19}H_{19}ClN_2O_3$: 358.1084; exact mass found: 358.1087; difference: +1.01 ppm.

1,5-diphenyl-3-(4-pivaloylphenyl)-6-oxotetrazane 7b

To a stirred solution of phenylhydrazine (0.22 mL, 0.24 g, 2.2 mmol) in ethanol (10 mL) was added α-chloroformylphenylhydrazone **S5** (0.40 g, 1.1 mmol), in small portions over 15 min. After

the addition was complete, the solution was heated to 55 °C and left to stir for 1 h. The solution began clear and became opaque as precipitate formed. The warm mixture was poured into ice cold water (30 mL). The off-white precipitate was filtered, dried *in vacuo* overnight and recrystallized in *n*-propanol to give **7b** as a white powder. Yield = 0.39 g, 80%. ^{1}H NMR (399.8 MHz, d_6-DMSO): δ 7.66 (d, 4H, $^{3}J_{HH}$ = 8 Hz, aryl C*H*), 7.62 (d, 2H, $^{3}J_{HH}$ = 8 Hz, aryl C*H*), 7.34 (t, 4H, $^{3}J_{HH}$ = 7 Hz, aryl C*H*), 7.10 (m, 4H, aryl C*H*), 6.33 (d, 2H, $^{3}J_{HH}$ = 9 Hz, N*H*), 5.43 (t, 1H, $^{3}J_{HH}$ = 9 Hz, C*H*), 1.33 (s, 9H, CH_3). ^{13}C{^{1}H} NMR (100.5 MHz, d_6-DMSO): δ 176.1, 156.4, 150.5, 142.7, 134.9, 128.0, 127.8, 123.1, 121.3, 121.1, 72.1, 38.3, 26.6. FT-IR (ranked intensity), KBr pellet: 692(7), 742(10), 757(11), 899(13), 918(12), 1118(1), 1165(4), 1310(8), 1200(9), 1373(3), 1500(5), CO tetrazane 1628(2), CO ester 1751(6), NH tetrazane 3241(14) cm^{-1}. Mass Spec. (EI, +ve mode): exact mass calculated for $C_{25}H_{26}N_4O_3$: 430.2005; exact mass found: 430.2011; difference: 1.39 ppm. Anal. Calcd. (%) for $C_{25}H_{26}N_4O_3$: C, 69.75; H, 6.09; N, 13.01. Found: C, 69.41; H, 6.21; N, 12.93.

1,5-diphenyl-3-(4-pivaloylphenyl)-6-oxoverdazyl 8b

This procedure was adapted from a report published by Hicks and coworkers.[10] Celite (0.10 g) and Ag_2CO_3 (0.19 g) were combined in methanol (10 mL) and stirred for 10 min. Tetrazane **7b** (0.15 g, 0.35 mmol) was then added to the suspension and the mixture was left to stir for 16 h at 20 °C. The solution turned a dark red colour and darkened as the reaction proceeded. To the mixture was added dichloromethane to dissolve the product and a gravity filtration was performed to remove Celite/Ag. The solid was recrystallized in methanol/H_2O (9:1) to give **8b** as a dark red solid. Yield = 1.40 g, 94%. FT-IR (ranked intensity) KBr pellet: 689 (1), 749 (9), 1113 (2), 1161 (6), 1201 (5), 1249 (8), 1485 (7), CO verdazyl 1702 (3), CO ester 1746 (4), 2974 (10)

cm^{-1}. UV-vis (CH_2Cl_2): λ_{max}: 563 nm (ε = 1,980 M^{-1} cm^{-1}), 317 nm (ε = 11,760 M^{-1} cm^{-1}), 258 nm (ε = 24,730 M^{-1} cm^{-1}). Mass Spec. (EI, +ve mode): exact mass calculated for $C_{25}H_{23}N_4O_3$: 427.1770; exact mass found: 427.1757; difference: –3.00 ppm. Anal. Calcd. (%) for $C_{25}H_{23}N_4O_3$: C, 70.24; H, 5.42; N, 13.11. Found: C, 70.24; H, 5.46; N, 13.00.

Additional Figures and Discussion

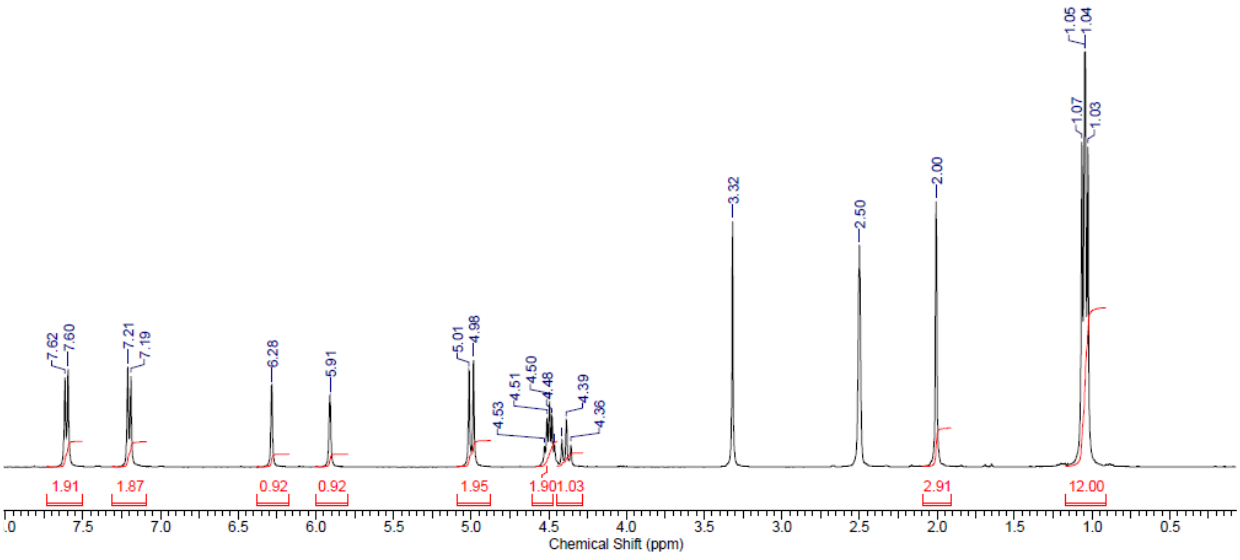

Fig. S1 ^{1}H NMR spectrum of tetrazane monomer **4a** in d_6-DMSO.

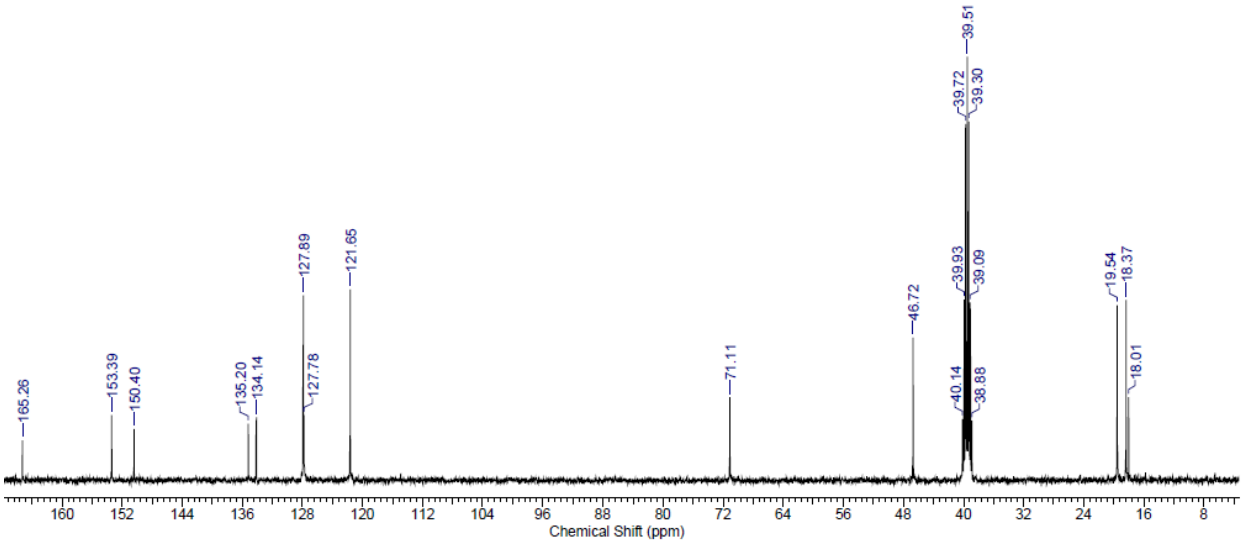

Fig. S2 ^{13}C{^{1}H} NMR spectrum of tetrazane monomer **4a** in d_6-DMSO.

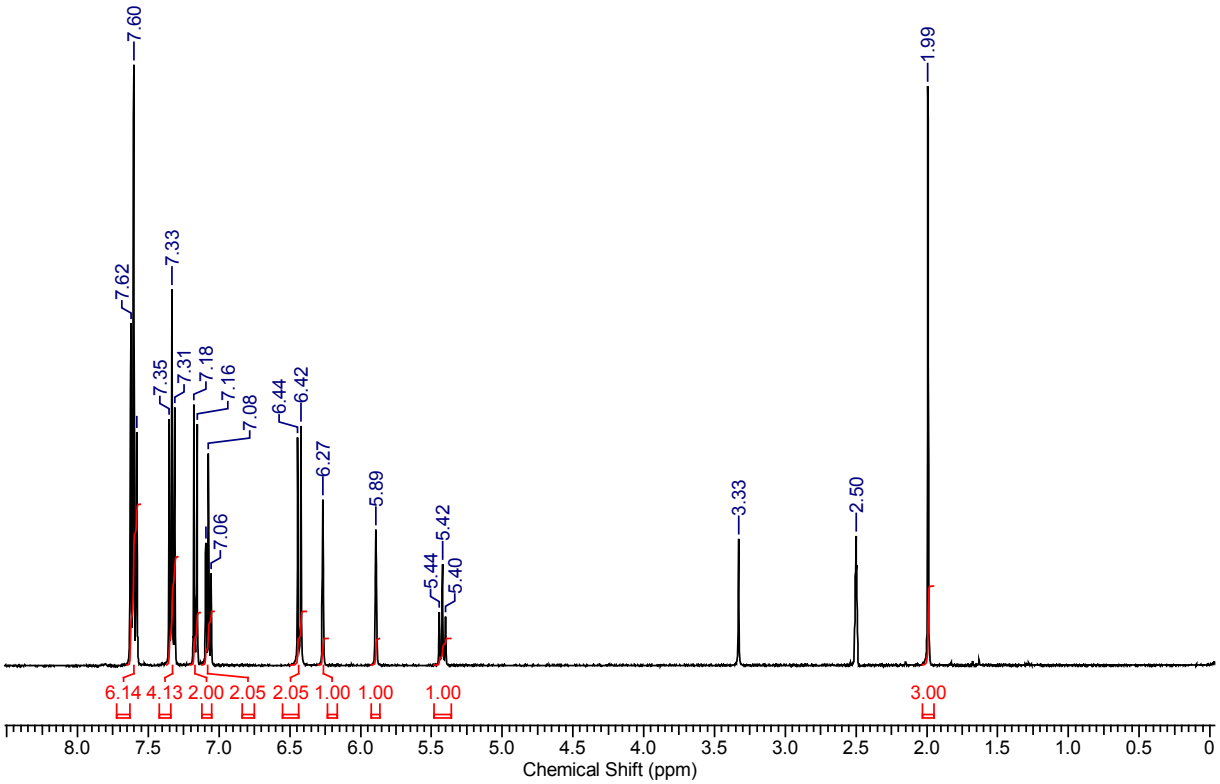

Fig. S3 ^{1}H NMR of tetrazane monomer **4b** compound in d_6-DMSO.

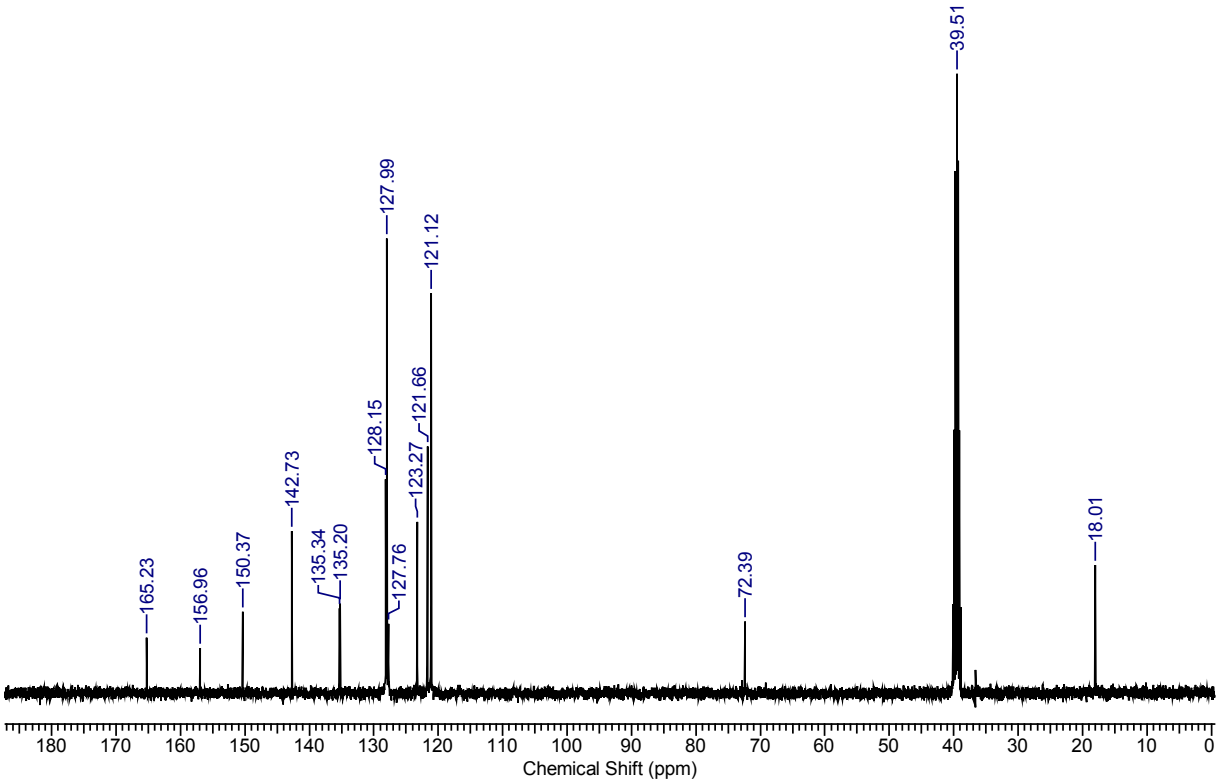

Fig. S4 ^{13}C{^{1}H} NMR tetrazane monomer **4b** in d_6-DMSO.

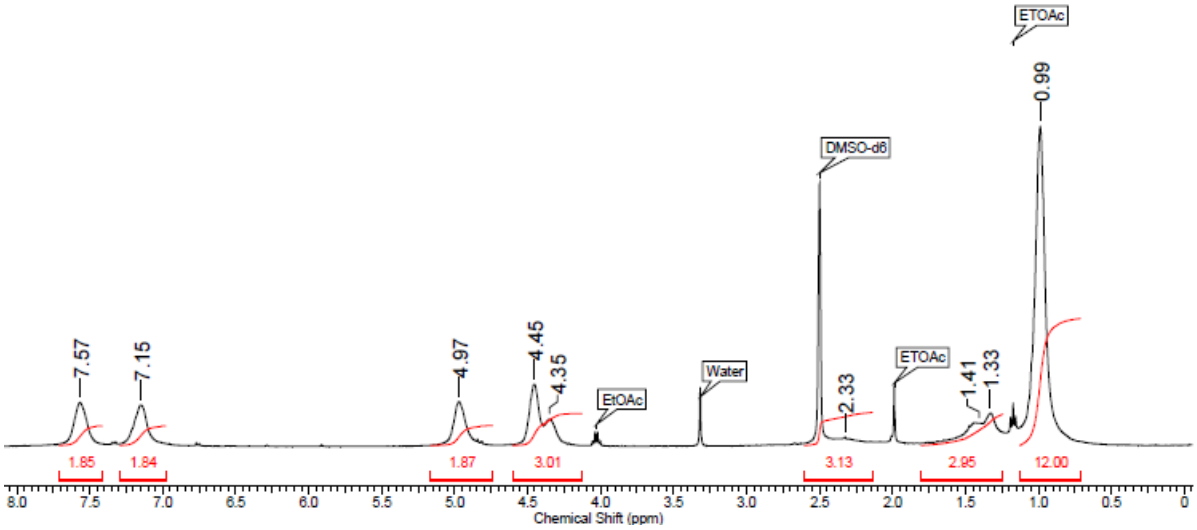

Fig. S5 ^{1}H NMR spectrum of tetrazane polymer **5a** in d_6-DMSO.

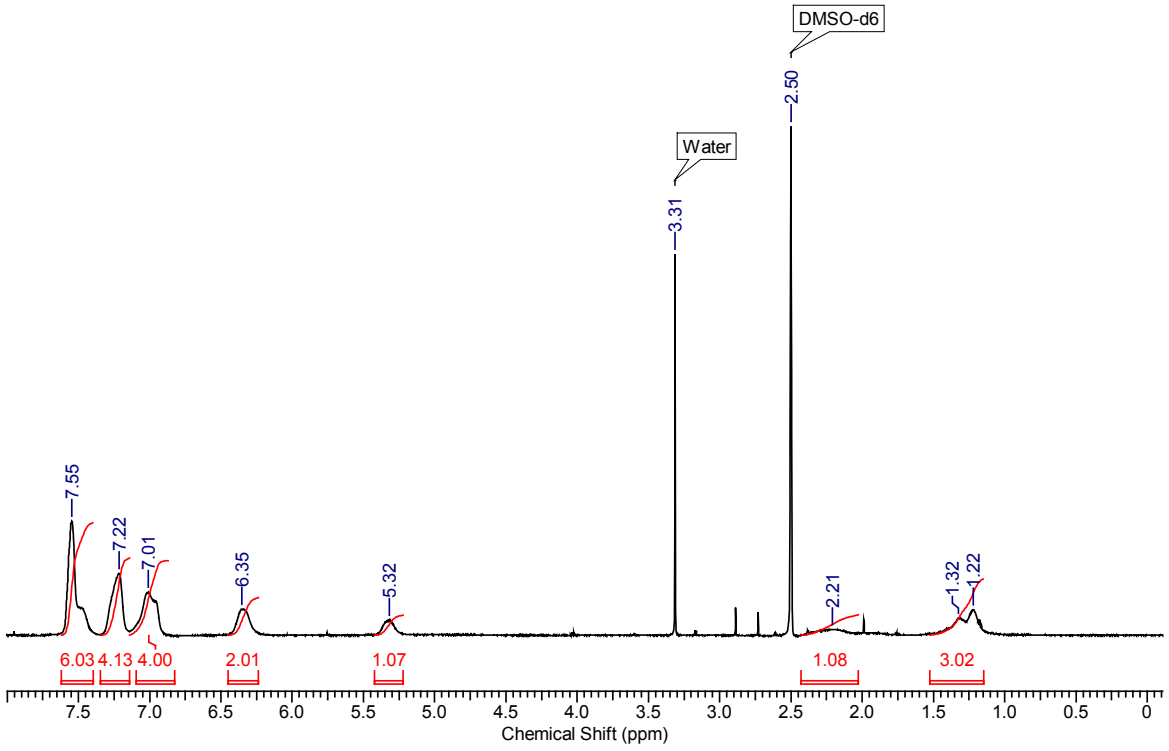

Fig. S6 ^{1}H NMR spectrum of tetrazane polymer **5b** in d_6-DMSO.

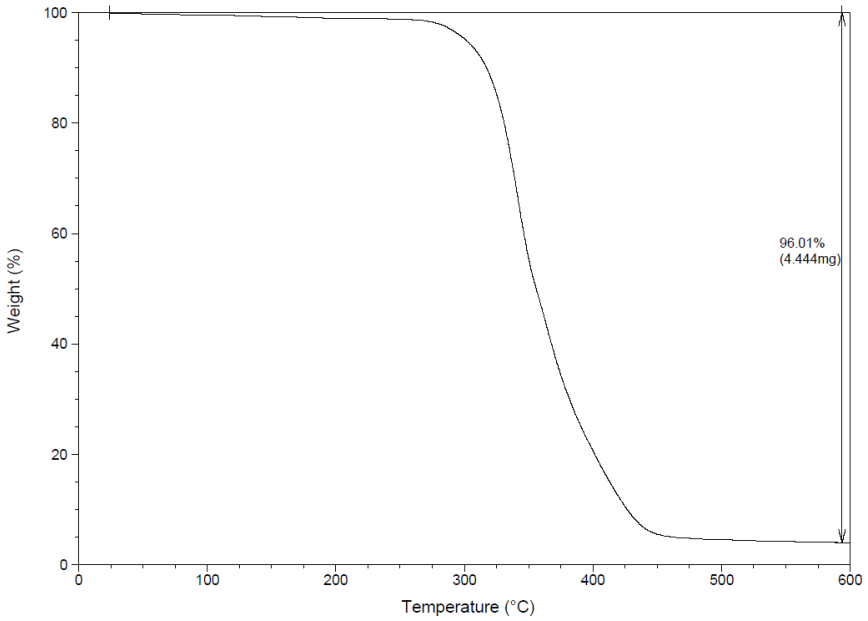

Fig. S7 TGA trace for tetrazane polymer **5a**.

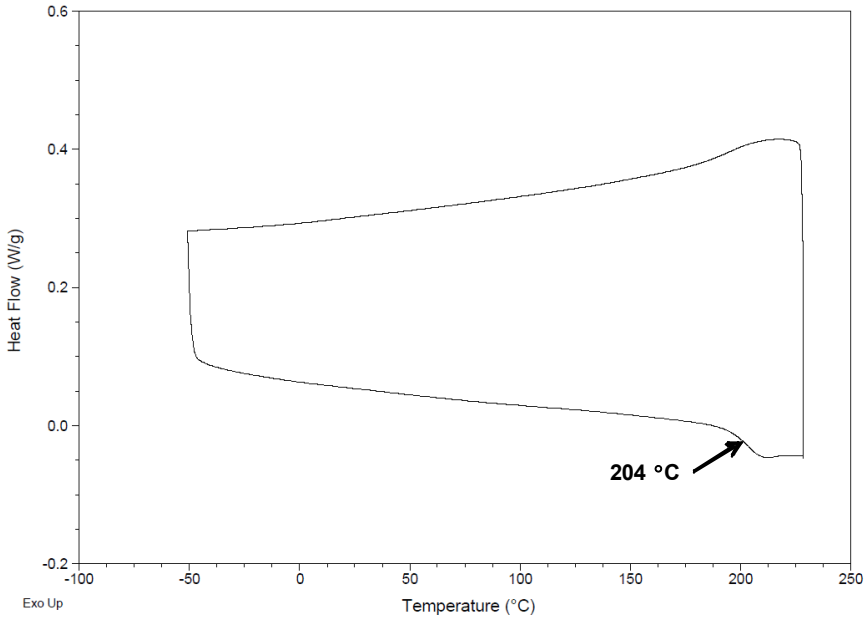

Fig. S8 DSC thermogram for tetrazane polymer **5a**.

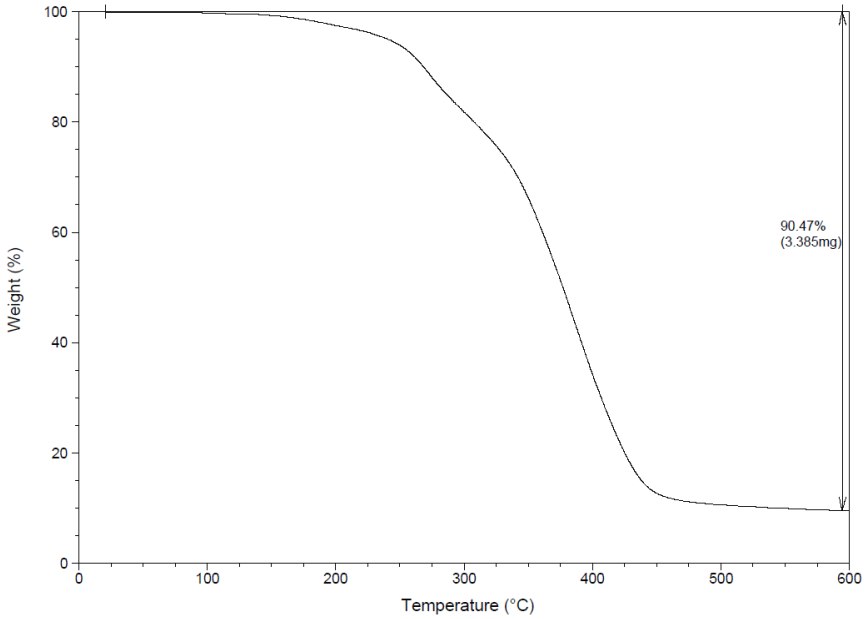

Fig. S9 TGA trace for 6-oxoverdazyl polymer **6a**.

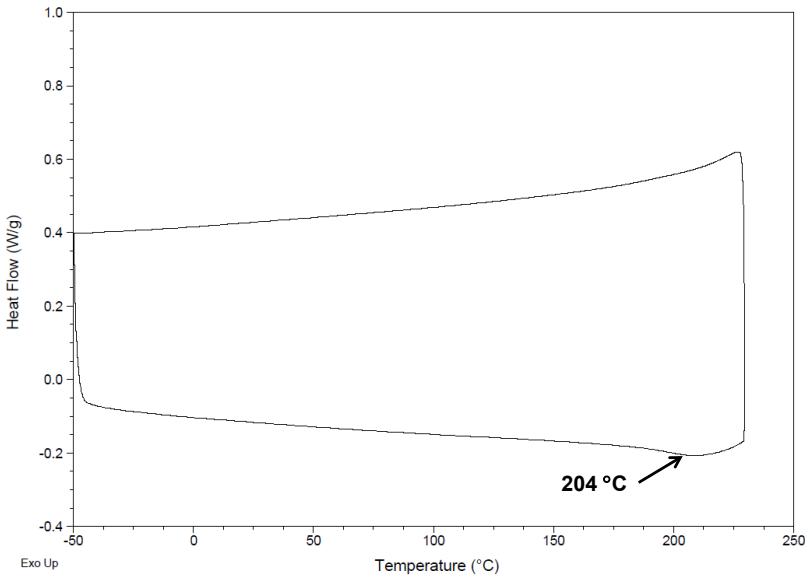

Fig. S10 DSC thermogram of 6-oxoverdazyl polymer **6a**.

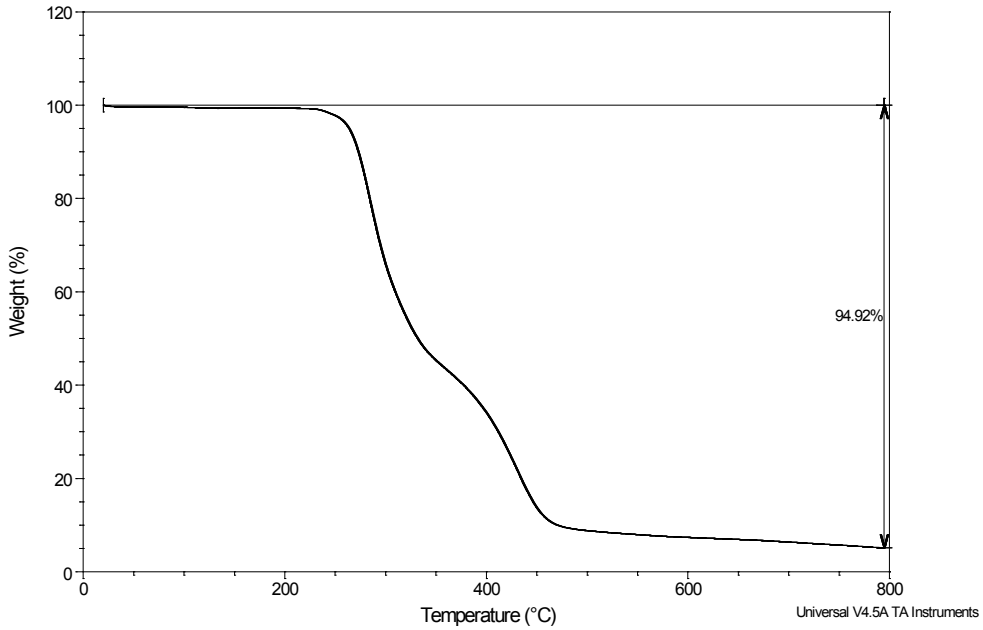

Fig. S11 TGA trace for tetrazane polymer **5b**.

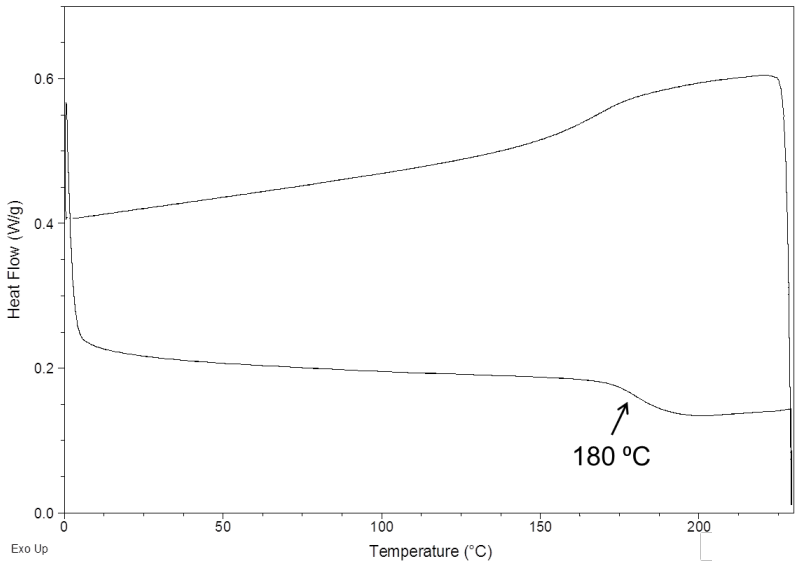

Fig. S12 DSC thermogram of tetrazane polymer **5b**.

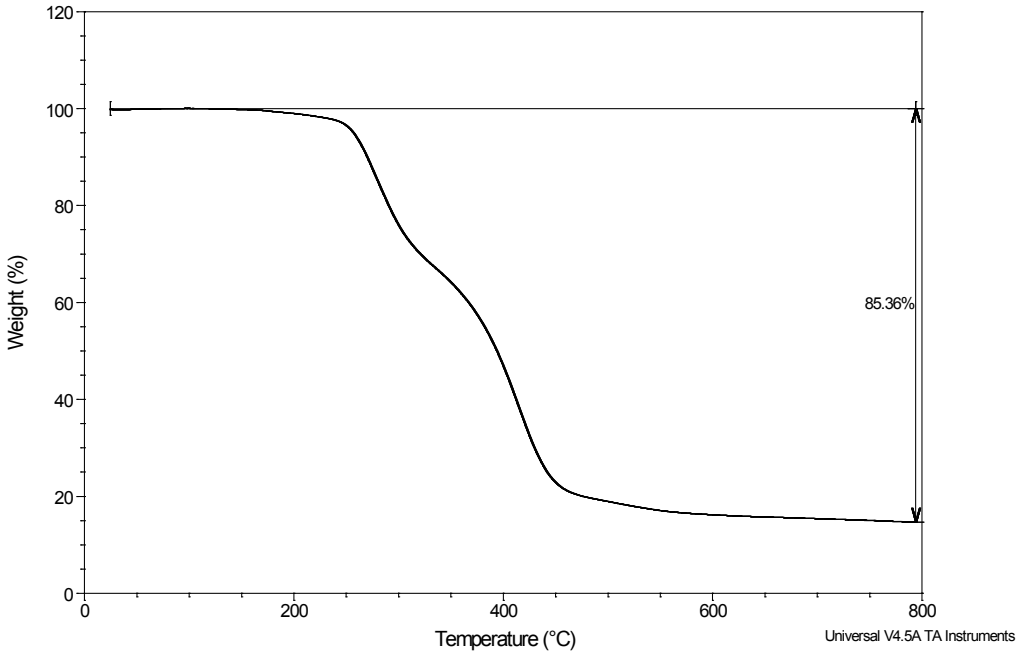

Fig. S13 TGA trace for 6-oxoverdazyl polymer **6b**.

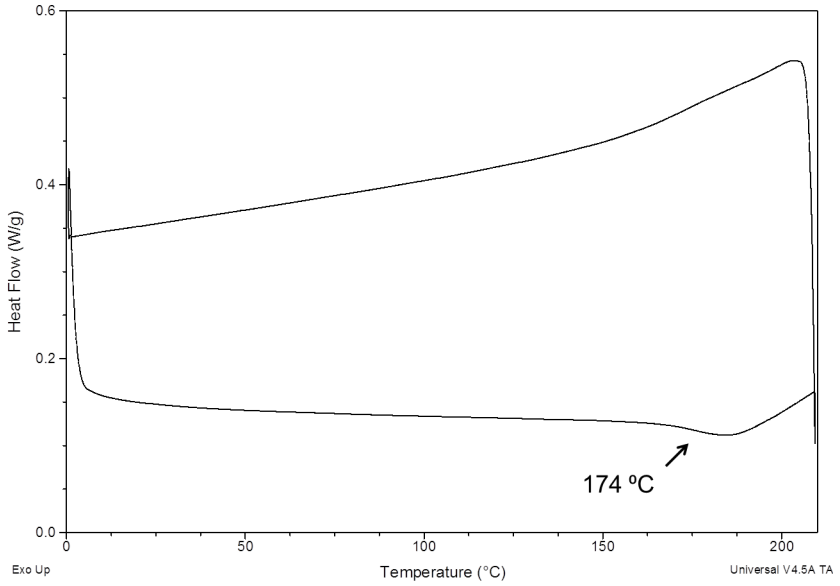

Fig. S14 DSC thermogram of 6-oxoverdazyl polymer **6b**.

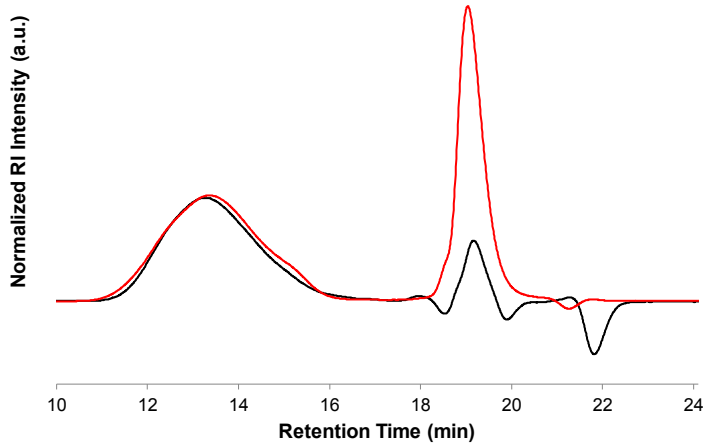

Fig. S15 Normalized GPC traces for tetrazane polymer **5a** (black) and 6-oxoverdazyl polymer **6a** (red) recorded in DMF containing 10 mM LiBr and 1% (v/v) triethylamine at 85 °C. The fluctuations between 17 and 23 min arise due to changes in RI associated with sample injections.

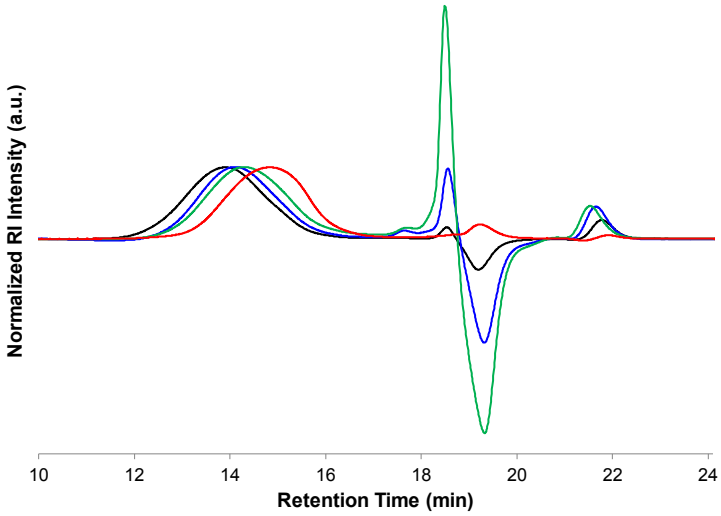

Fig. S16 Normalized GPC traces for tetrazane polymer **5b** (black), tetrazane polymer **5b** after air oxidation for 24 h (blue), tetrazane polymer **5b** after air oxidation for 48h (green), and 6-oxoverdazyl polymer **6b** (red), recorded in DMF containing 10 mM LiBr and 1% (v/v) triethylamine at 85 °C. The fluctuations between 17 and 23 min arise due to changes in RI associated with sample injections.

Discussion of GPC Results

The polymers presented in this paper, including tetrazane polymers **5a,b** and 6-oxoverdazyl polymers **6a,b**, all exhibit drastically different solubility profiles. In general, the tetrazane polymers are soluble only in highly polar solvents while 6-oxoverdazyl polymers are soluble in a wide range of solvents. We were unable to obtain reproducible GPC data for our polymers in THF due to the lack of solubility of tetrazane polymers **5a,b**. However, we were able to obtain reproducible GPC data for all of our polymers in DMF containing 10 mM LiBr and 1% (v/v) NEt_3 at 85 °C using conventional calibration (vs. polystyrene) for the determination of molecular weight distributions. Tetrazane polymer **5a** and 6-oxoverdazyl polymer **6a** gave rise to very similar GPC traces (Fig. S15). Tetrazane polymer **5b** and 6-oxoverdazyl polymer **6b** did not behave in the same way (Fig. S16). We initially suspected that the chemical oxidation of tetrazane polymer **5b** using *p*-benzoquinone as an oxidant in refluxing THF/MeOH may have resulted in chain scission. However, upon closer inspection of the distributions observed for **5b** and **6b**, we hypothesized that it was highly unlikely that chain scission had occurred based on the remarkably similar shape and width of the distributions (PDI = 1.48 for **5b**, PDI = 1.46 for **6b**). To further probe this hypothesis, we allowed the GPC solution used for the analysis of **5b** to stand in air to partially oxidize. The sample, which becomes a random tetrazane/6-oxoverdazyl copolymer upon partial oxidation, was analyzed after 24 h and after 48 h of air exposure (Fig. S16). As the radical content in the polymer increased with time, the centre of the GPC distributions shifted to longer retention times and the shape and width of the distributions did not change significantly (PDI = 1.40 for **5b** after 24 h in air, PDI = 1.50 for **5b** after 48h in air). The center, shape, and width of the GPC traces obtained for 6-oxoverdazyl polymer **6b** after standing in air did not change. The difference in molecular weights observed for tetrazane polymer **5b** and 6-oxoverdazyl polymer **6b** appears to arise due to limitations associated with the comparison of

polymers with substantially different solubility profiles using conventional calibration GPC. It is likely that each of our polymers interact very differently with the solvent system and size-exclusion columns employed, and that their properties match those of the polystyrene standards employed to different extents [specifically the relationship between molecular weight and radius of gyration (R_g) in the solvent system employed].

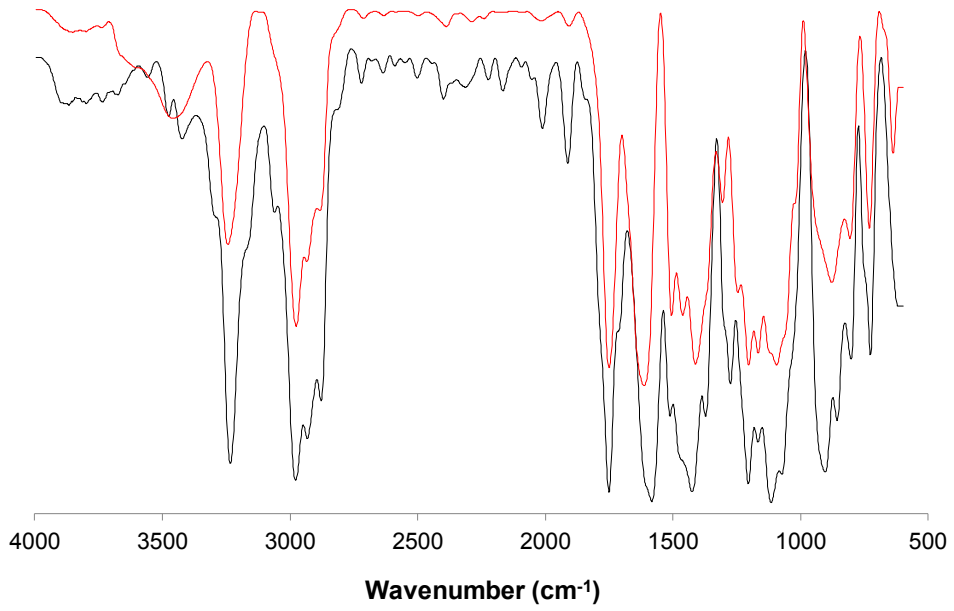

Fig. S17 IR spectra of tetrazane polymer **5a** (red) and tetrazane **7a** (black) recorded as KBr pellets. The baselines have been offset for ease of comparison.

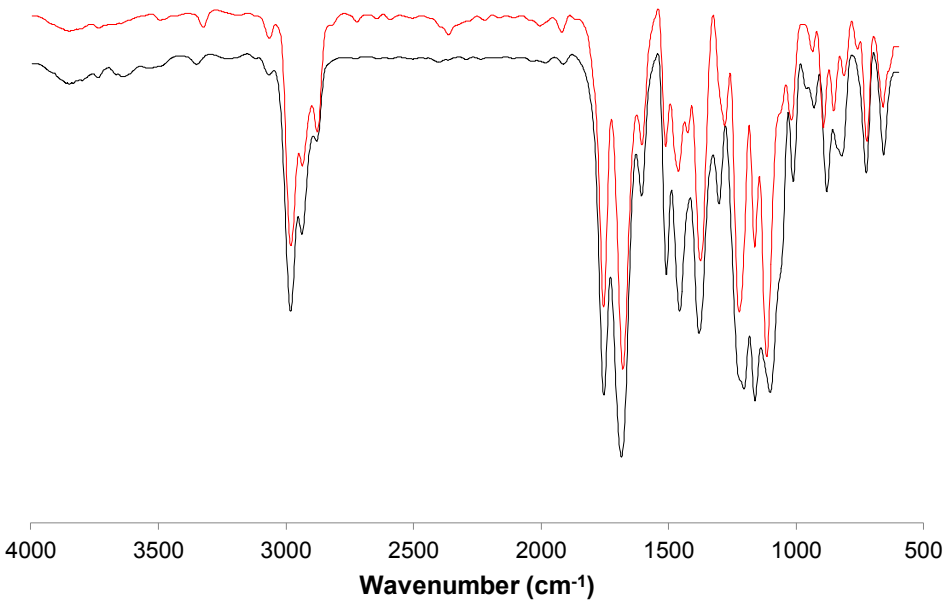

Fig. S18 IR spectra of 6-oxoverdazyl polymer **6a** (black) and 6-oxoverdazyl **8a** (red) recorded as KBr pellets. The baselines have been offset for ease of comparison.

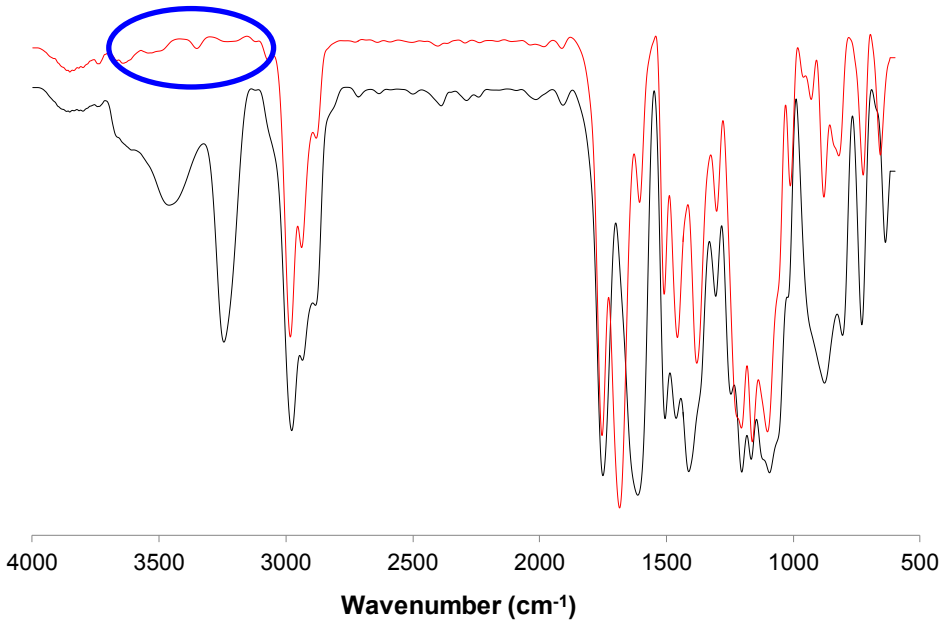

Fig. S19 IR spectra for tetrazane polymer **5a** (black) and 6-oxoverdazyl polymer **6a** (red) recorded as KBr pellets. The blue ellipse highlights the region of the spectrum where NH stretches would be expected. The baselines have been offset for ease of comparison.

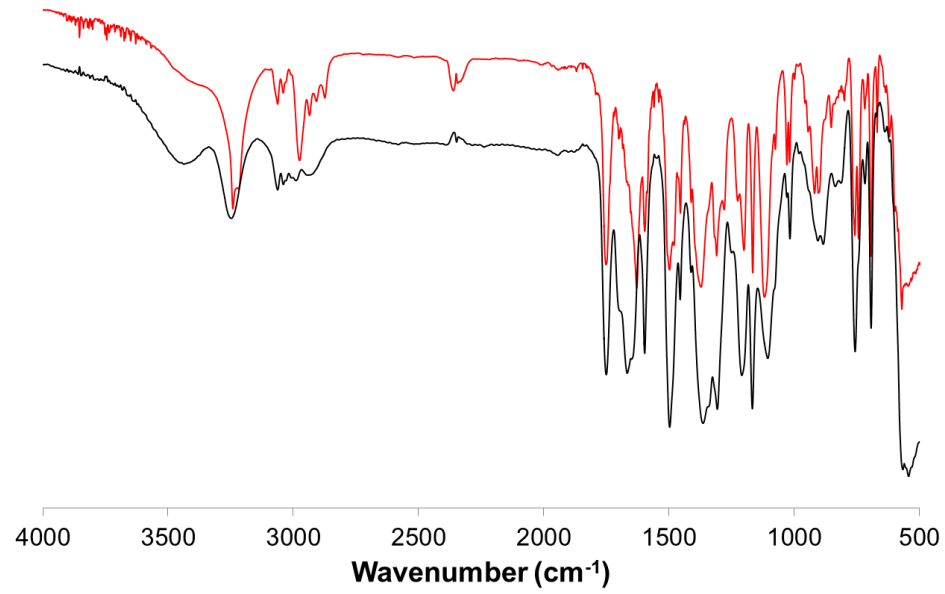

Fig. S20 IR spectra for tetrazane polymer **5b** (black) and tetrazane **7b** (red) recorded as KBr pellets. The baselines have been offset for ease of comparison.

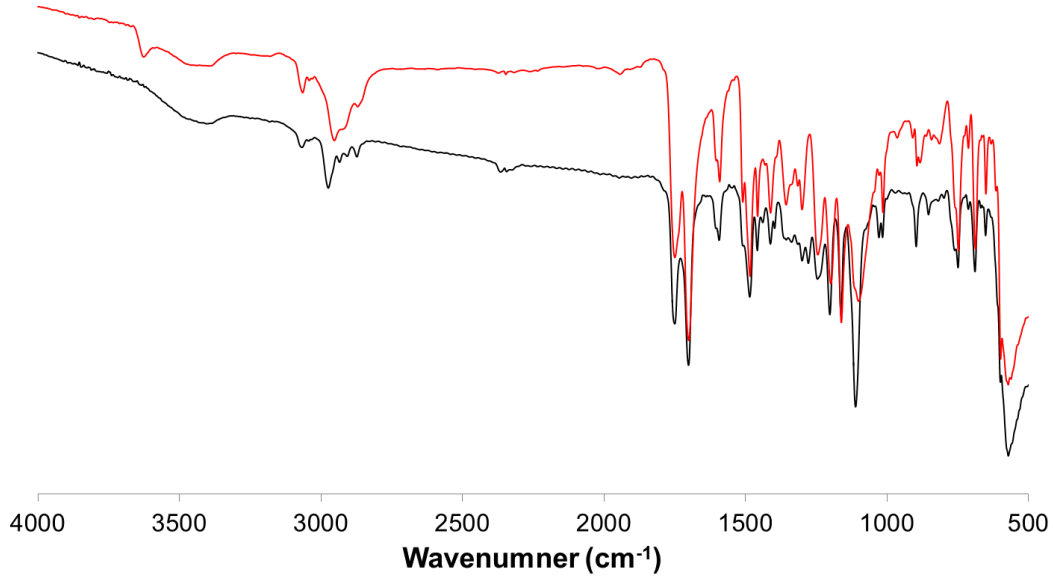

Fig. S21 IR spectra of 6-oxoverdazyl polymer **6b** (red) and 6-oxoverdazyl **8b** (black) recorded as KBr pellets. The baselines have been offset for ease of comparison.

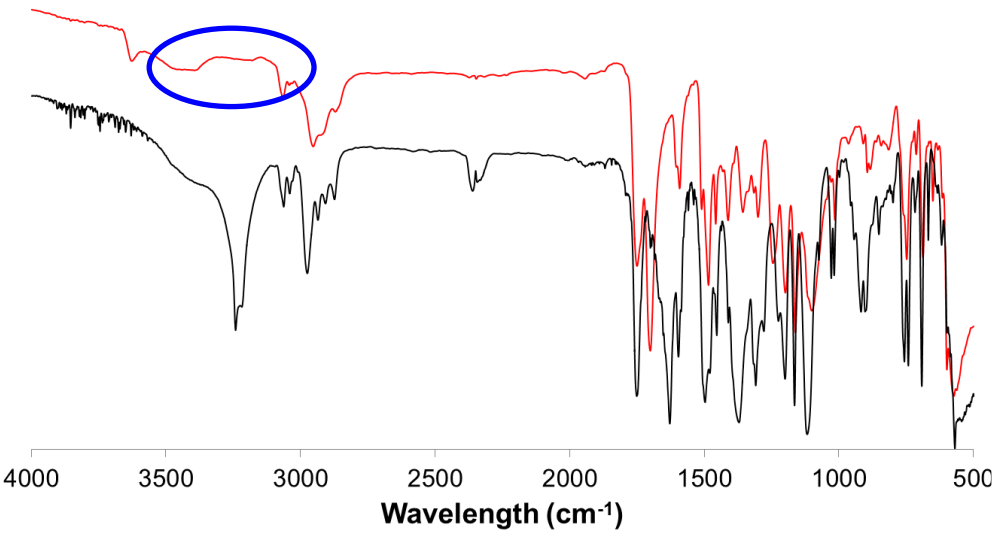

Fig. S22 IR spectra for tetrazane polymer **5b** (black) and 6-oxoverdazyl polymer **6b** (red) recorded as KBr pellets. The blue ellipse highlights the region of the spectrum where NH stretches would be expected. The baselines have been offset for ease of comparison.

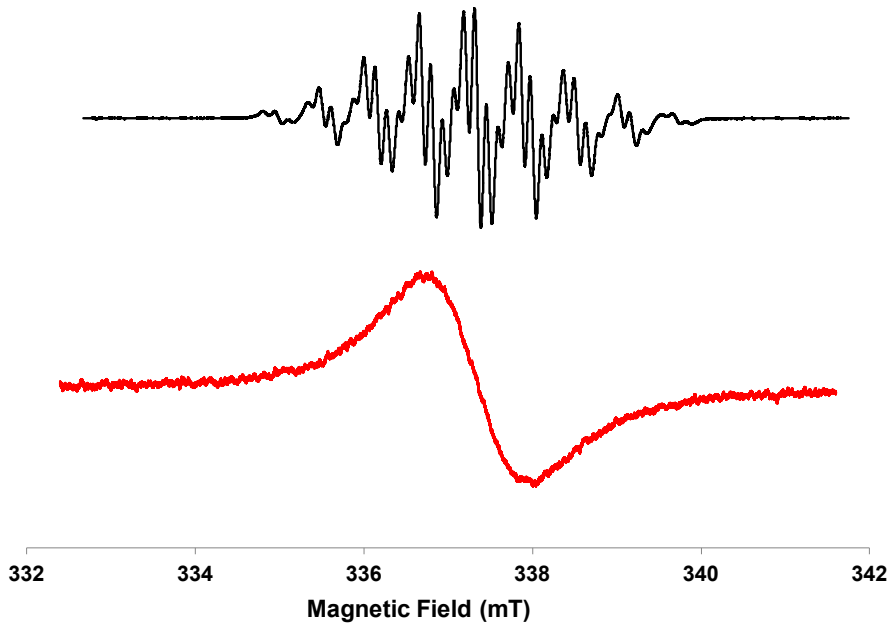

Fig. S23 EPR spectra of 6-oxoverdazyl **8a** (g = 2.0043, black) and 6-oxoverdazyl polymer **6a** (g = 2.0050, red) in dichloromethane. See Fig. S24 for simulation of the spectrum of 6-oxoverdazyl **8a**.

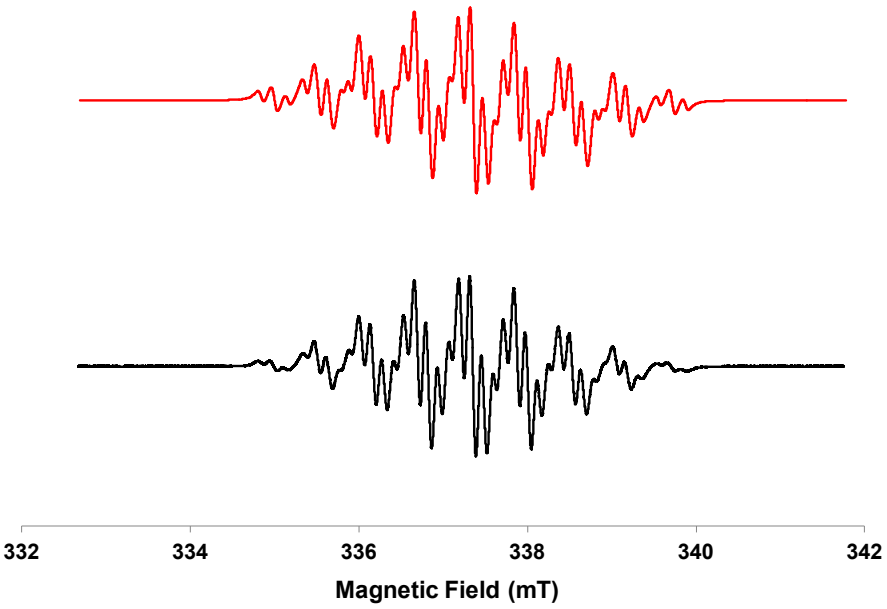

Fig. S24 Simulated (top, red) and collected (bottom, black) EPR spectra of 6-oxoverdazyl **8a** in dichloromethane. Parameters used for simulation: g = 2.0043, line width = 0.85 mT, $a_{N1,5}$ = 0.533 mT, $a_{N2,4}$ = 0.656 mT, a_H = 0.132 mT.

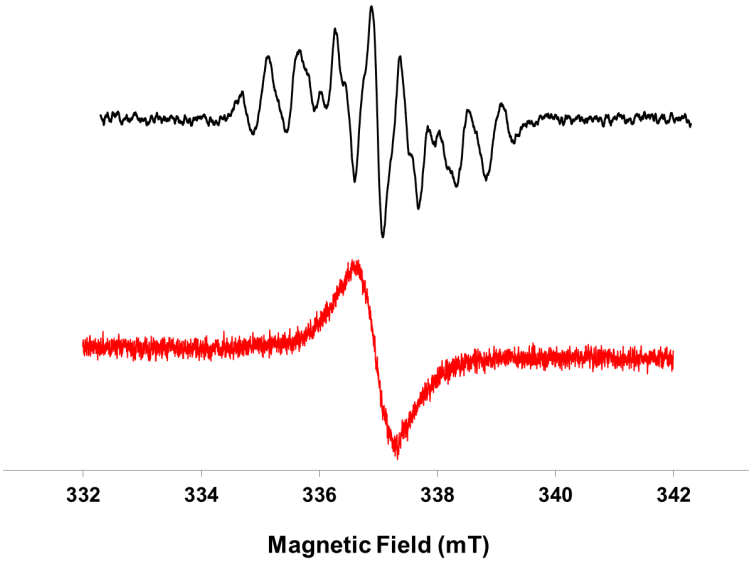

Fig. S25 EPR spectra of 6-oxoverdazyl **8b** (g = 2.0038, black) and 6-oxoverdazyl polymer **6b** (g = 2.0043, red) in dichloromethane. See Fig. S26 for simulation of the spectrum of 6-oxoverdazyl **8b**.

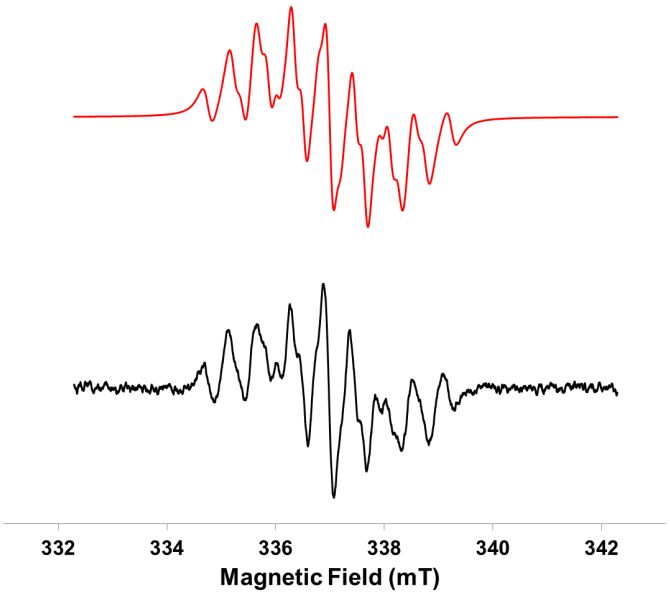

Fig. S26 Simulated (top, red) and collected (bottom, black) EPR spectra of 6-oxoverdazyl **8b** in dichloromethane. Parameters used for simulation: g = 2.0038, line width = 0.20 mT, $a_{N1,5}$ = 0.645 mT, $a_{N2,4}$ = 0.475 mT.

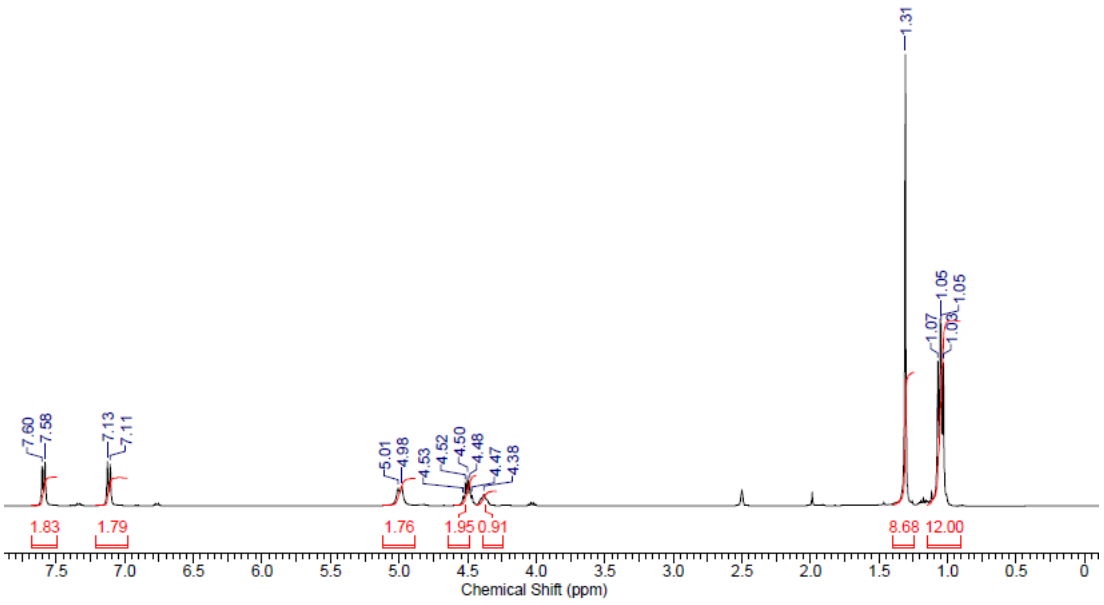

Fig. S27 ^{1}H NMR spectrum of tetrazane **7a** in d_6-DMSO.

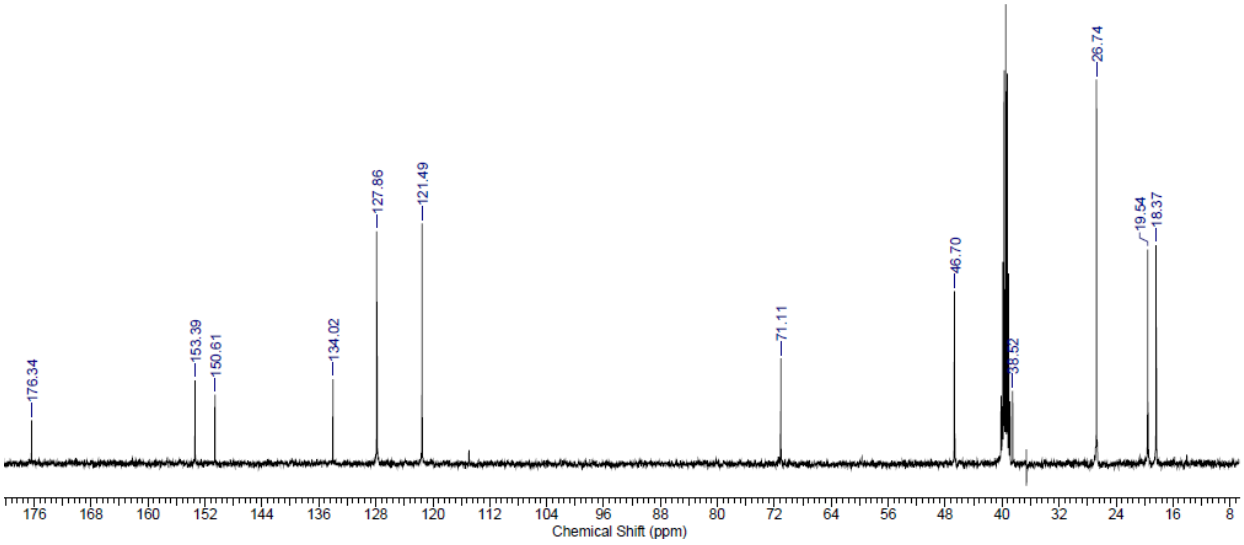

Fig. S28 $^{13}C\{^{1}H\}$ NMR spectrum of tetrazane **7a** in d_6-DMSO.

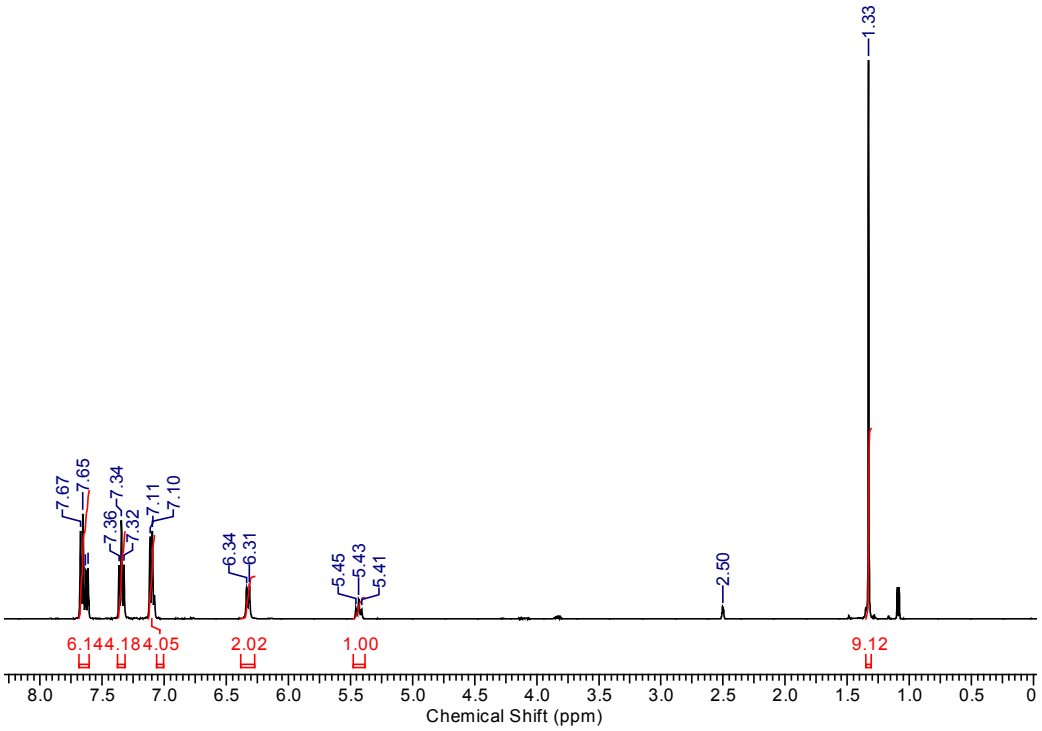

Fig. S29 ^{1}H NMR of tetrazane **7b** in d_6-DMSO.

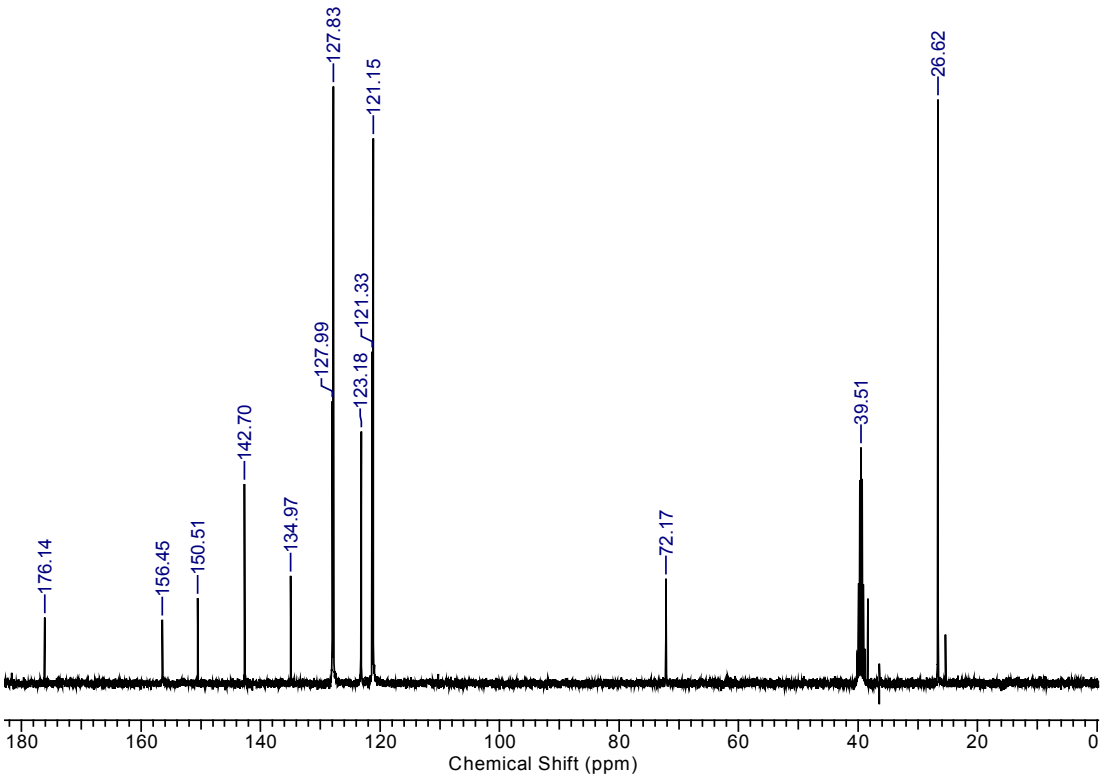

Fig. S30 $^{13}C\{^{1}H\}$ NMR tetrazane **7b** in d_6-DMSO.

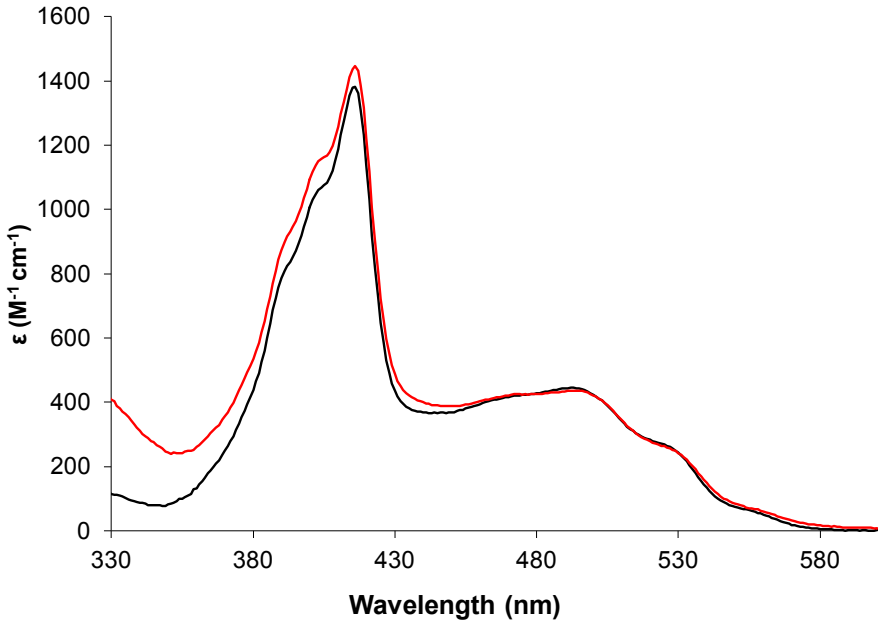

Fig. S31 UV-vis absorption spectra of 6-oxoverdazyl polymer **6a** (red) and model 6-oxoverdazyl **8a** (black) recorded in CH_2Cl_2.

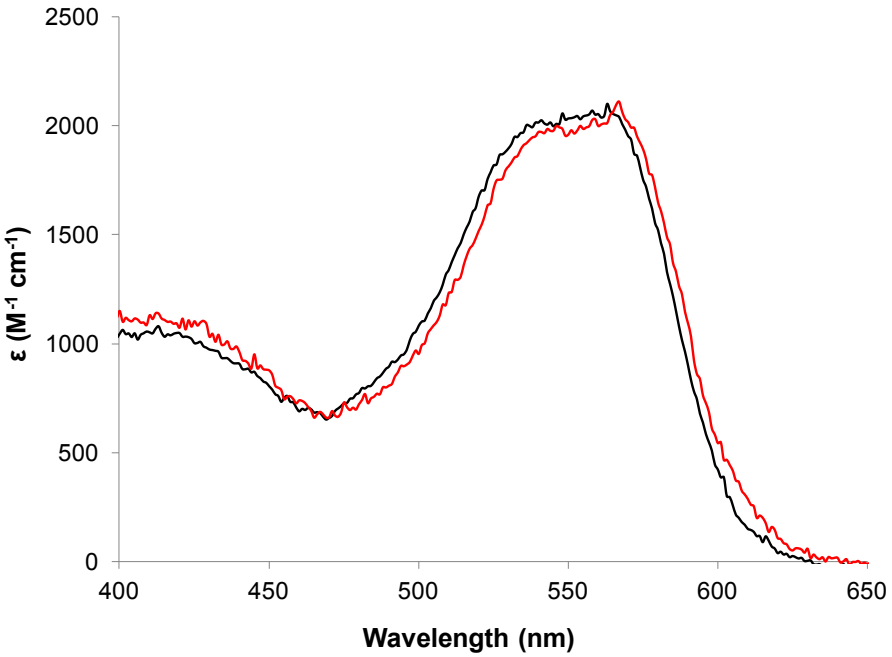

Fig. S32 UV-vis absorption spectra of 6-oxoverdazyl polymer **6b** (red) and model 6-oxoverdazyl **8b** (black) recorded in CH_2Cl_2.

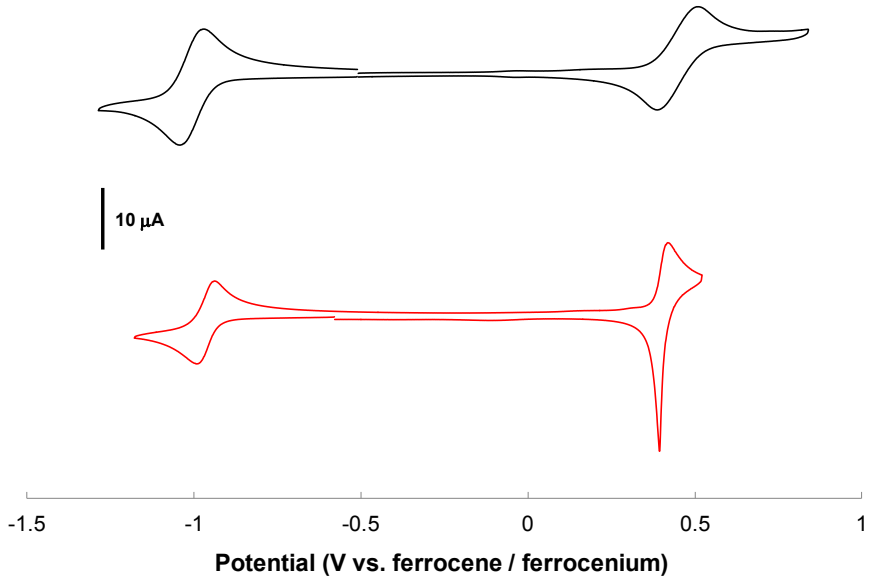

Fig. S33 CVs of 6-oxoverdazyl **6b** (black) and 6-oxoverdazyl polymer **8b** (red) recorded at scan rate 50 mV s^{-1} in THF solutions containing 1 mM analyte and 0.1 M tetrabutylammonium hexafluorophosphate as supporting electrolyte.

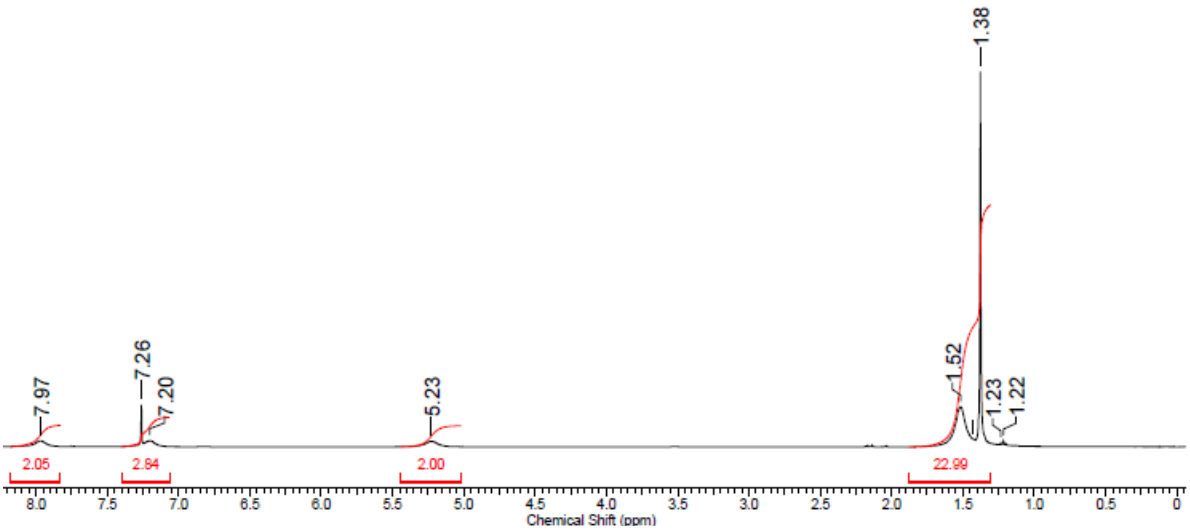

Fig. S34 ^{1}H NMR spectrum of tetrazinium cation **9a** in $CDCl_3$.

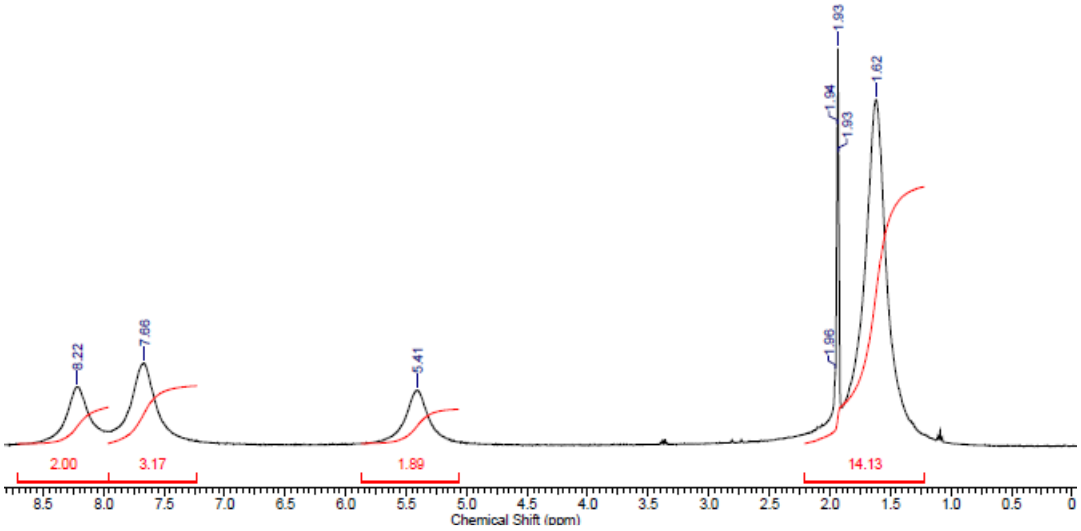

Fig. S35 ^{1}H NMR spectrum of tetrazinium cation **9c** in CD_3CN at –40 °C.

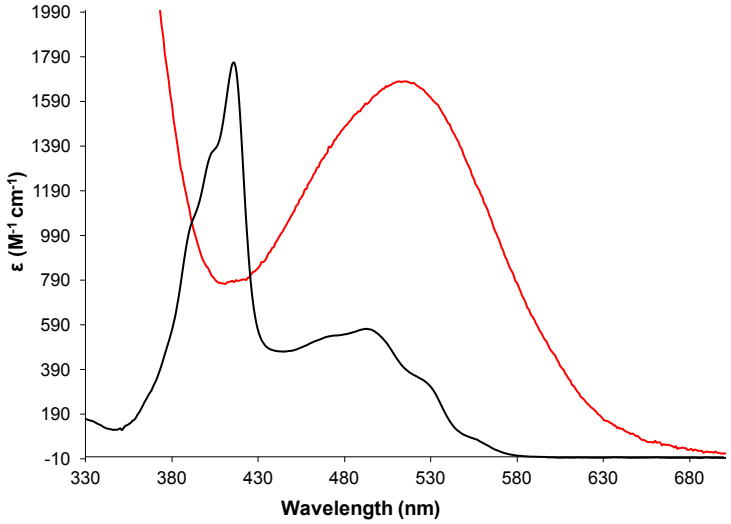

Fig. S36 UV-Vis absorption spectra of 6-oxoverdazyl **8a** (black) and tetrazinium cation **9a** (red) recorded in CH_2Cl_2.

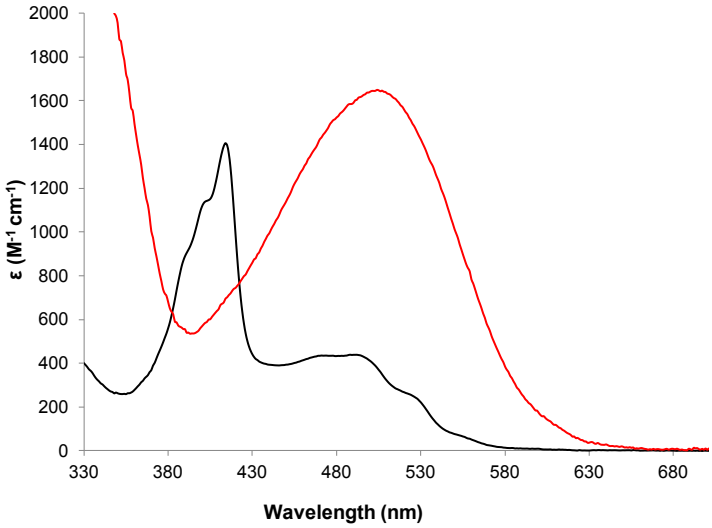

Fig. S37 UV-Vis absorption spectra of 6-oxoverdazyl **8c** (black) and tetrazinium cation **9c** (red) recorded in CH_2Cl_2.

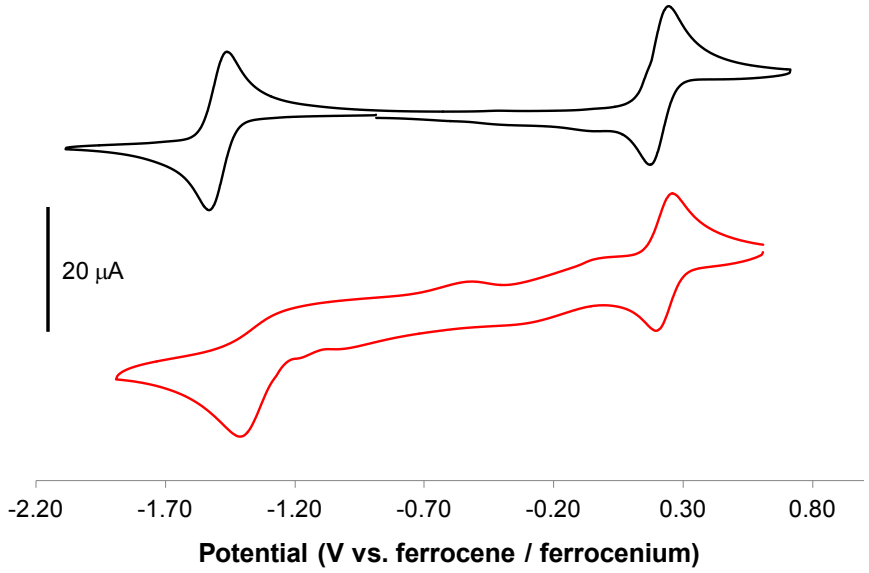

Fig. S38 CVs of 6-oxoverdazyl **8a** (black) and tetrazinium cation **9a** (red) recorded at scan rate 100 mV s^{-1} in THF solutions containing 1 mM analyte and 0.1 M tetrabutylammonium hexafluorophosphate as supporting electrolyte. The reduction wave is irreversible due to the consumption of electrochemically generated anion by excess cation **10a** in solution.

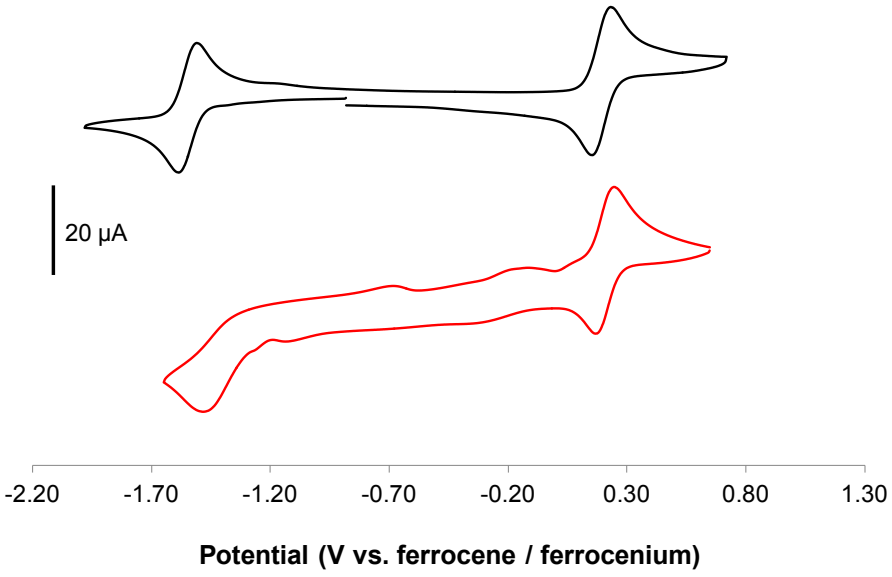

Fig. S39 CVs of 6-oxoverdazyl **8c** (black) and tetrazinium cation **9c** (red) recorded at scan rate 100 mV s^{-1} in THF solutions containing 1 mM analyte and 0.1 M tetrabutylammonium hexafluorophosphate as supporting electrolyte. The reduction wave is irreversible due to the consumption of electrochemically generated anion by excess cation **9c** in solution.

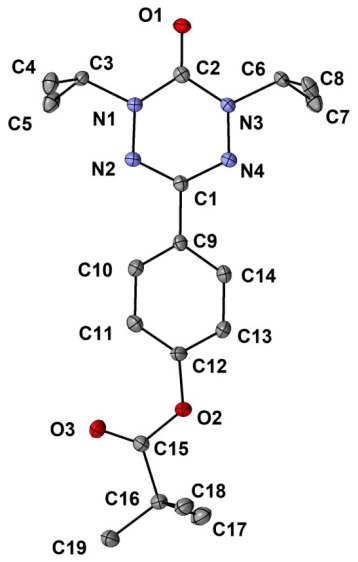

Fig. S40 Solid-state structure of **8a**. Thermal ellipsoids are shown at 50% probability level. Hydrogen atoms have been omitted for clarity.

Table S2 Selected bond lengths (Å) and angles (°) for 6-oxoverdazyl **8a**.

bonds and angles	**8a**
N1-N2, N3-N4	1.365(1), 1.368(1)
C1-N2, C1-N4	1.333(1), 1.331(1)
N1-C2, N3-C2	1.379(1), 1.379(1)
N1-N2-C1, N3-N4-C1	115.11(8), 115.24(7)
N2-C1-N4	126.66(8)
N1-C2-N3	113.74(8)

References

1 B. García-Acosta, F. García, J. M. García, R. Martínez-Máñez, F. Sancenón, N. San-José and J. Soto, *Org. Lett.*, 2007, **9**, 2429–2432.

2 L. Jiménez-González, S. García-Muñoz, M. Álvarez-Corral, M. Muñoz-Dorado and I. Rodríguez-García, *Chem. Eur. J.*, 2007, **13**, 557–568.

3 E. C. Paré, D. J. R. Brook, A. Brieger, M. Badik and M. Schinke, *Org. Biomol. Chem.*, 2005, **3**, 4258–4261.

4 V. Chemistruck, D. Chambers and D. J. R. Brook, *J. Org. Chem.*, 2009, **74**, 1850–1857.

5 J. B. Gilroy, S. D. J. McKinnon, P. Kennepohl, M. S. Zsombor, M. J. Ferguson, L. K. Thompson and R. G. Hicks, *J. Org. Chem.*, 2007, **72**, 8062–8069.

6 F. Sharifi, R. Bauld and G. Fanchini, *J. Appl. Phys.*, 2013, **114,** 144504.

7 R. Schlaf, H. Murata and Z. H. Kafafi, *J. Electron Spectrosc. Relat. Phenom.*, 2001, **120**, 149–154.

8 (a) G. M. Sheldrick, *Acta Cryst.*, 2008, **A64**, 112–122; (b) M. C. Burla, R. Caliandro, M. Camalli, B. Carrozzini, G. L. Cascarano, C. Giacovazzo, M. Mallamo, A. Mazzone, G. Polidori, R. Spagna, *J. Appl. Cryst.*, 2012, **45**, 357–361.

9 R. Milcent, G. Barbier, S. Capelle and J.-P. Catteau, *J. Heterocycl. Chem.*, 1994, **31**, 319–324.

10 J. B. Gilroy, S. D. J. McKinnon, B. D. Koivisto and R. G. Hicks, *Org. Lett.*, 2007, **9**, 4837–4840.